

AD-A195 637

RE-EVALUATION OF THE STABILITY OF LARGE CONCRETE
STRUCTURES ON ROCK WITH. (U) EIDGENÖSSISCHE TECHNISCHE
HOCHSCHULE LAUSANNE (SWITZERLAND). K KOVARI ET AL.

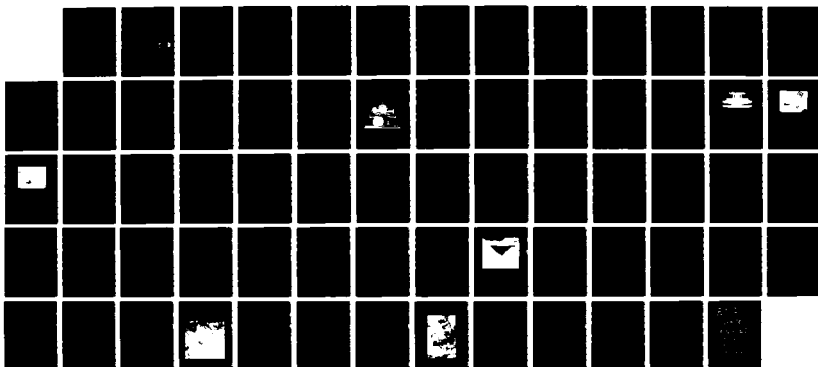
1/1

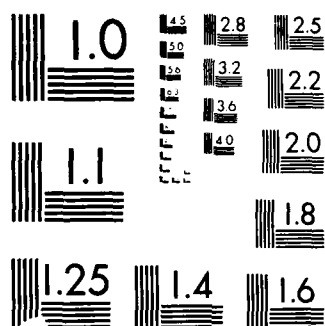
UNCLASSIFIED

APR 88 R/D-5611-EN-01 DAJA45-86-M-0489

F/G 13/2

NL





RESOLUTION TEST CHART
 U.S. GOVERNMENT PRINTING OFFICE: 1963 O

DTIC FILE COPY

2

TECHNICAL REPORT

RE-EVALUATION OF THE STABILITY OF LARGE CONCRETE STRUCTURES ON ROCK WITH EMPHASIS ON EUROPEAN EXPERIENCE

AD-A195 637

by

K. Kovari and P. Fritz
Swiss Federal Institute of Technology
Zürich, Switzerland

April 1988
Final Report

DTIC
ELECTE
MAY 24 1988
S D
CAD

DISTRIBUTION STATEMENT A

Approved for public release
Distribution Unlimited

Prepared for DEPARTMENT OF THE ARMY
UNITED STATES ARMY RESEARCH DEVELOPMENT
AND STANDARDIZATION GROUP

Under Contract No. DAJA4S-86-M-0489

ABSTRACT

The sliding stability of a rock mass forming the foundation or the abutments of concrete dams, of a natural slope, or of a cut cannot be measured directly but merely conjectured. One knows, however, the nature of the mechanisms which may lead to a failure and, conversely, remedial measures which may enhance the existing stability. Attention must be paid to sliding hazard if the presence of adversely oriented discontinuities with considerable persistence is evident, if movements take place in the rock mass, if high water pressures are measured in faults, and/or if wet spots at critical areas of a slope or downstream of the dam foundation are known to occur. A change in the flow rate of the drains can also be an indication of an unsafe condition. The most effective way and in many instances the only practical solution to increase stability against sliding is to prevent or to eliminate the occurrence of excessive water pressure below the foundation or in faults. The second possibility involves reinforcements by anchoring and shear keys, and the third is removal or placement of rock masses and concrete in critical areas. The problem which arises in practice is to weigh correctly the different pieces of information relating to the assessment of the degree of stability.

The aim of the authors is to draw attention to recent developments in stability analysis and in rock mass behaviour monitoring which may be helpful, by themselves or in combination, in dealing with the problems encountered in practice. These means are helpful in increasing available information and in assigning a relative value to it. However, whatever the amount of information that has been collected, there will always be areas of ignorance and therefore room for interpretation. Future efforts should therefore be directed to further develop simple means of investigation and to draw conclusions from incidents and observed behaviour, and not to attempt to formalize the procedure to assess the sliding stability of the structures.



- i -

Accession For	
NES CRA&I	<input checked="checked" type="checkbox"/>
DTIC TAB	<input type="checkbox"/>
Unannounced	<input type="checkbox"/>
Justification	
By <i>per form 50</i>	
On (date)	
Availability Codes	
Dist	Avail and/or Served
<i>A-1</i>	

RE-EVALUATION OF THE STABILITY OF LARGE CONCRETE STRUCTURES ON ROCK WITH EMPHASIS ON EUROPEAN EXPERIENCE

CONTENTS

INTRODUCTION

Aims and Scope	1
The Concept of Structural Behaviour and Safety	3
Particularities of the Re-evaluation of Sliding Stability of Existing Dams	5

ROCK MECHANICS CONSIDERATIONS

Discontinuities and Their Relevance	7
Rock Mass Deformability	8
Rock Mass Permeability	9

MEANS OF MONITORING STRUCTURAL BEHAVIOUR

Physical Quantities of Interest	10
The Concept of "Linewise Observation"	11
High Precision Deformation Measurements	12
High Precision Water Head Measurements	18
Interpretation of Measurements	24

STABILITY ANALYSIS

Introduction	28
Simple Plane Failure	30
Simple Wedge Failure	35
Polygonal Plane failure	41

CASE HISTORIES

Kölnbrein Arch Dam	45
Valle di Lei Arch Dam	52
Albigna Gravity Dam	54
Example of a Creeping Slope	60

REFERENCES

62

Introduction

AIMS AND SCOPE

Foundation failure due to sliding is one of the predominant causes of failure of concrete dams. (ICOLD, 1987). Sliding can occur along the contact between concrete and rock or along planes of weakness deep in the rock foundation or abutments. (Fig. 1). Failure may occur during the first impoundment or even after many years of operation. A particular problem arises from reservoir slopes instabilities which may generate reservoir waves overtopping the dam. It has been observed that most, if not all concrete dam disasters to this date have happened under static load conditions (von Thun, 1977).

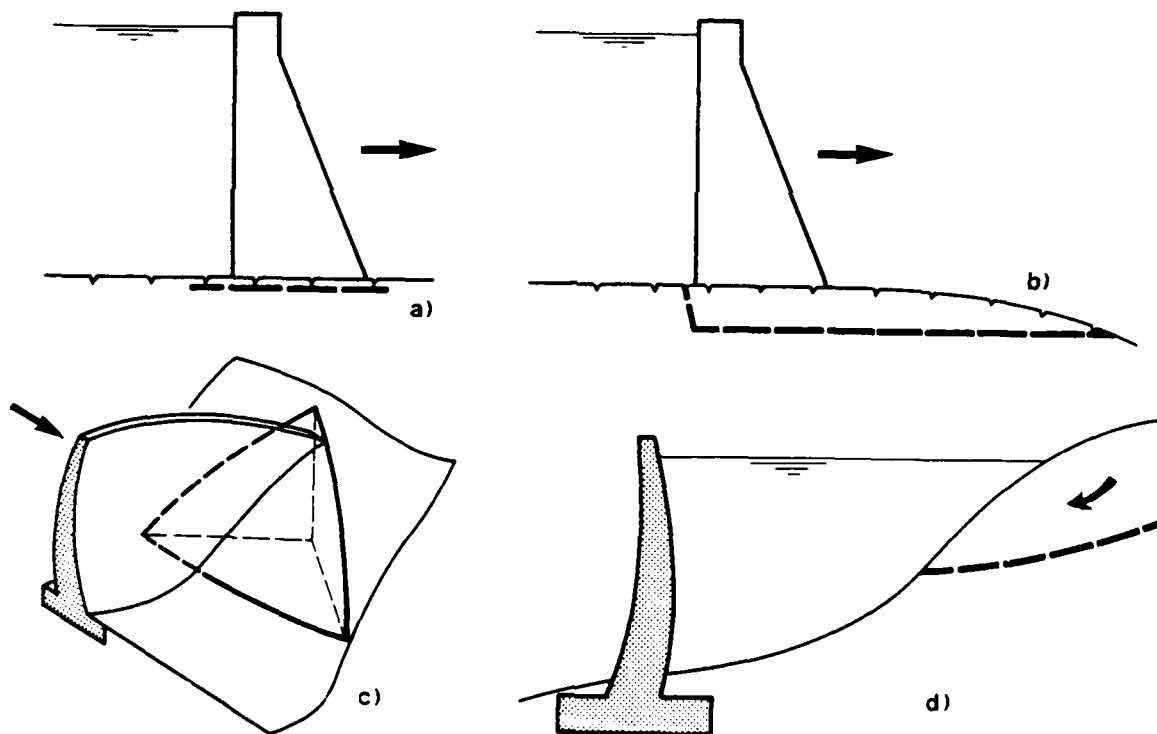


Fig. 1 Typical cases of potential sliding
 a) Sliding of a block along the rock-concrete contact
 b) Sliding surface deep in the foundation rock
 c) Sliding of a wedge in the dam abutment (after P.Londe)
 d) Instability of reservoir banks

This report deals solely with one aspect of safety, namely the problem of sliding stability of concrete dams. The approach to this problem is necessarily a rock mechanics one, indicating how analytical and observational procedures can supplement each other.

The re-evaluation of the sliding stability of an existing dam generally proceeds in different stages. In the first stage, all existing data are reviewed and analysed, and field observations are carried out. If the results of these first-stage activities reveal no potential sliding, no further investigations are needed. The dam, however, will continue to be subjected to the "normal" surveillance and maintenance program. If the stability of the dam is considered questionable, then field explorations, numerical analyses and specific "behaviour monitoring" should be initiated. This second stage of investigation relies on the facts, impressions or hypotheses which have been obtained in the preceding stage. Any safety re-evaluation program depends heavily upon the conditions specific to the site, on the available records, but also on the background and experience of the investigators involved. On the other hand, there are many facts which are common to all safety evaluations. Apart from site exploration and material testing, there are two powerful means at the disposal of the investigating engineer: analytical methods to check the factor of safety against sliding and specific behaviour monitoring. In the following, emphasis is placed on these tools, showing recent developments and the nature of the problems to which they can successfully be applied.

The analytical approach starts with the identification of potential sliding bodies, according to suspected or clearly recognised planes of weakness in the rock. Recognition of unfavourably oriented main discontinuities is crucial. The location, orientation, water pressure, extension and shear strength of such critical discontinuities will be used in the analysis. Based on the first preliminary results, previously suspected failure modes for sliding might be completely ruled out, and others may be retained for further consideration. Unfortunately, inherent uncertainties concerning the safety level may still remain. In this case, "behaviour monitoring" can yield additional information regarding the safety of the structure.

"Behaviour monitoring" is an integral part of any dam safety program. There are two reasons for this: first, if there is no major change discernable in the behaviour of the dam, in its foundation or in its abutments, during an observation period, it can be assumed that a constant safety level prevails; the monitoring thus confirms existing safety. Secondly, failure, as a rule, is progressive. Even if a concrete dam already fails as a result of the first reservoir impoundment, it should be possible to detect progressive stages of failure by means of careful monitoring during the filling of the reservoir. Monitoring is a powerful help in detecting developments in the dam which may lead to partial or complete failure. In this way, failure can be prevented or its effects minimised by timely initiation of preplanned emergency measures.

One has to keep in mind, however, that "behaviour monitoring" has its limitations as well. It does not give quantitative information about how close the potential sliding mass is to the condition of failure. In other words, the factor of safety against sliding can never be measured directly. Due to its idealised concept, it can only be conjectured from empirical data and determined by calculation.

Another point of interest concerns the extent and sensitivity of the performed "behaviour monitoring". A poor program of measurements may result in misleading interpretations. The layout and the sensitivity of the measurements should always consider the envisaged aim. Another shortcoming of monitoring is the difficulty in extrapolating the influence of unprecedented loading cases on the safety of the dam. Examples for this are earthquakes and malfunctioning drains. Such predictions must be reached by analytical procedures.

The authors are aware of the costs involved in the re-evaluation of the safety of an existing dam and of the conflicting aspects of the reliability of the results and the available budget. Optimum resource allocation is a difficult but essential part of the task. The common practice of a staged approach is strongly recommended. The sooner a potential sliding problem is recognised, the greater the number of options available to the engineer for dealing with the problem. The highest costs result from remedial measures and/or from operation of a dam at lower reservoir levels. Early recognition of conditions which might threaten the stability of a dam is therefore not only of importance to maintain an adequate safety standard but also to enable the engineer to work out the most economical remedial measures.

THE CONCEPT OF STRUCTURAL BEHAVIOUR AND SAFETY

Structural behaviour means the response of the dam and its foundation to loads and ageing, e.g. cyclic impounding and emptying of the reservoir, change in temperature, earthquakes, material deterioration, dissolution etc. The development of cracks and open joints in concrete and rock and the appearance of erosion and piping, among other factors, may be visible indicators of an unexpected behaviour. Deformations, piezometric heads, seepage volumes and possibly anchor forces are the most important quantities which may be measured directly. Stresses in concrete and rock are not suitable quantities because of local material inhomogeneities and because they can not be measured directly. The absolute values of the measured quantities are seldom crucial for the safety assessments; much more important are their change in time for the same loading conditions. Such changes in the structural behaviour may be an indicator of the initiation of a progressive failure.

To what extent the structural behaviour of a dam should be observed and monitored depends largely on the previous records. However, for all dams above a given height and a given reservoir capacity, a minimal regular surveillance and monitoring effort is required by legislation. A complete monitoring history, starting with the construction and followed by the first and subsequent impoundments, should ideally exist for all dams. The more is known about the normal behaviour of a dam, the easier it is to determine evidences of anomalies and take early preventive and remedial action.

The concept of safety is a matter of continuous debate. Fortunately, the lack of a widely accepted formalised safety concept does not seem to affect the safe operation of a dam. Nevertheless, it gives rise to difficulties in communication among the engineers. Without attempting to add to the discussions on safety concepts, we would just like to recall the two ways leading to the judgements on dam safety, particularly with respect to sliding. Both ways aim at characterizing safety by the margin which separates the actual working conditions from those of failure.

The first approach is an attempt to handle the problem in an analytical way. The factor of safety is defined as the ratio of the shear strength to the available shear stress acting on the potential sliding surface. An equivalent formulation states that the factor of safety is a number by which the strength properties can be reduced, before failure occurs (ICOLD, 1978). Safety against sliding is therefore measured as a reserve of strength.

The vagueness arising from the different sources of uncertainty (shear strength parameters, persistency of the discontinuities, uplift, etc.) and the fact that the absolute value of the factor of safety may never be observed in the field, have led some engineers to the conclusion that the factor of safety should not have any absolute significance. It should only act as a sensitivity index showing to what extent stability is affected by changes in the basic mechanical data adopted (Londe, 1973). A few remarks seem appropriate at this point. Unity (1.0) as the extreme value for the factor of safety is still of great importance: below it no equilibrium would be possible. Only values equal or greater than unity are therefore considered in practice. However, decisions on values for an "acceptable" factor of safety largely depend on (local) circumstances, e.g. selection of data for analysis, consequences of a failure, intensity and layout of monitoring program, etc. It is therefore not advisable to establish general rules for minimum required values of the factor of safety, even if they are grouped according to loading cases.

As was mentioned above, although dam monitoring yields quantitative information, it does not allow an absolute quantification of dam safety. Emphasis is placed here on the confirmation of the existing safety which is deemed to exist at the time of observation. Surveillance and monitoring thus ensure the maintenance of a given, although, as a rule, unknown level of safety. Many failures and accidents that have occurred in the past could have been avoided if proper measurements and observations had been made and if data had been expeditiously analysed (ICOLD, 1974). Remedial measures aim at restoring previous working conditions or at stopping developments which could lead to failure. Analytical investigations are usually required to discuss the influence of remedial measures on safety, thereby linking the observational and analytical approaches.

PARTICULARITIES OF THE RE-EVALUATION OF SLIDING STABILITY OF EXISTING DAMS

There are two problems with existing, mainly old dams, which make the evaluation of their safety more difficult than safety predictions for a new dam. First, the records of these dams are often incomplete or extremely poor. Secondly, one does not have the full range of options for site explorations that are available prior to and during the construction of a new dam. Consider, for example, the limited access to the foundation rock and to the ground surface in the water-filled reservoir. On the other hand, the simple fact that a dam has been and is still operating demonstrates its stability. That means that under the prevailing conditions, the factor of safety against sliding must be at least unity. Furthermore, behaviour monitoring is possible at prototype scale.

One has to keep in mind that the design and construction of older dams often come short of the quality that can presently be reached in dam construction. Data from recent dam incidents show clearly that older dams have experienced failure and accidents more frequently and with much worse consequences than well-engineered, modern dams built since 1940 (ASCE/USCOLD, 1975). Reports from older dam designs show that in some cases uplift was completely disregarded.

To emphasize the great influence of uplift forces Fig. 2 may serve. The dam shown was designed to have a factor of safety of 1.4 against sliding for typical sets of cohesion and angle of friction, but neglecting potential uplift forces (i.e. maximal uplift pressure $u_v=0$). However, taking into account uplift leads to a substantial decrease of the factor of safety. For a linear distribution and a maximal uplift pressure u_v which equals the horizontal water pressure u_h at the bottom of the dam, the factor of safety decreases to 1.3 and 1.0 respectively, depending on the shear strength parameters considered. It is interesting to note that the decrease of safety is more pronounced for smaller values of the cohesion than of the friction angle.

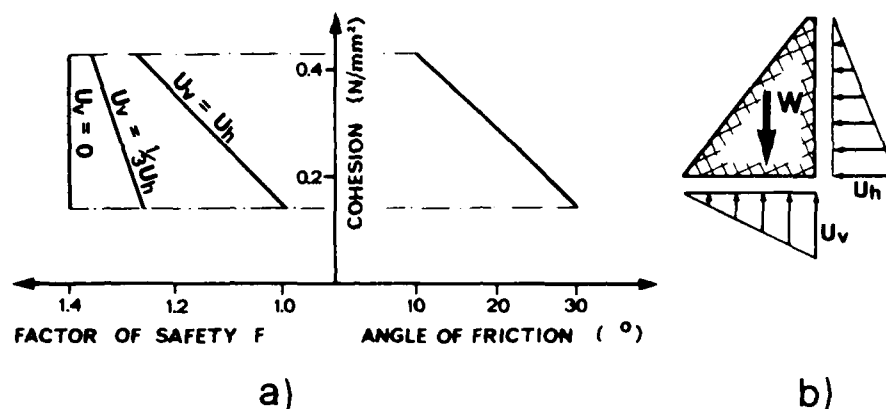


Fig. 2 Influence of uplift forces on factor of safety
 ($W = 32'500 \text{ kN}$, $u_h = 0.6 \text{ N/mm}^2$)
 a) Factor of safety
 b) Cross section

In such cases, or in cases of poor documentation, a comprehensive monitoring program should be initiated, with frequent readings in the starting phase, to establish a database which reflects the normal behaviour under variable operating conditions. Besides deformation, the most important quantities to be measured are the piezometric heads.

Rock Mechanics Considerations

The rock foundation and abutments of concrete dams must withstand the forces transferred by the structure (dam thrust, forces exerted by earthquakes etc.). They must also resist the seepage forces due to the difference in head caused by reservoir impounding or by rapid drawdowns of the reservoir water level. Deformability, strength and permeability of a rock mass are usually closely related to the nature of the discontinuities present in the rock. There is a relation between these factors which must be properly understood when analysing failures of and incidents to dams and when interpreting the results of field measurements and visually detected anomalies.

DISCONTINUITIES AND THEIR RELEVANCE

The presence of discontinuities in a rock mass largely determines its response to changes in stress. Thus, its overall deformability, its safety against sliding and the percolation of water may be decisively influenced by known or hidden joints and other planes of weakness. Even if the structure of the rock mass and the nature of its discontinuities are carefully explored and described, the uncertainties with respect to joint persistence, fracture network, and strength properties may be significant. Those discontinuities which may exhibit differential movements (opening, closing and shear displacement) are of special interest. They will be referred to as active joints, in contrast to potential planes of weakness. The identification of active joints in the foundation rock, in the dam abutment or in the slopes of the reservoir may be crucial whenever signs of unexpected behaviour are evident. It may also be important to know to which extent the concrete is cracked and how these cracks respond to the reservoir water level.

In order to assess the sliding stability of a gravity dam, the abutments of an arch dam or the reservoir slopes, only discontinuities with adverse orientation and large extension are of immediate relevance. For example, in cases of gravity dams and concrete gravity intake structures, detection of near-horizontal mylonite seams and shear zones are crucial. In such cases, plane failure mechanisms will be predominant, i.e. sliding on one plane or on several planes having the same dip direction. In steep valleys with arch dams, it is often the wedge type of instability which causes main concern.

Discontinuities with small degrees of persistence do not influence sliding stability directly, except in the cases where they occur regularly and in unfavourable combinations. In such cases, they can lead to stepped plane or stepped wedge failure. Generally existing intact material bridges, however, bring about an apparent cohesion which resists sliding and makes stepped failure often less critical than continuous shear zones or seams.

Experience shows that very often the existence of discontinuities with adverse orientation is only revealed during the construction of a dam, although very careful exploration work might have been carried out in the design stage. The reason for this is that fillings of joints are often washed out during boring, thereby making the recognition of joints difficult or impossible.

Once the existence of major discontinuities with adverse orientation has been identified, the main problem involves the assessment or determination of the shear strength parameters. Filling, asperities (amplitudes and inclinations), undulation and intact rock strength are decisive. The way of combining these factors to values of friction and cohesion needed in analytical investigations, not to mention the further refinement of methods of differentiating between peak and residual strength values, are by no means trivial and still present a matter of discussion. Indeed, the engineering community is also divided as to how it applies these values. Some reject considering residual values at all, others use them for exceptional loading cases only (e.g. earthquakes), and others admit lower factors of safety when considering residual values. In this connection, it may be pointed out once again that safety concepts should not be standardized. The final acceptance of values of safety factors also depends necessarily on subjective arguments and it should therefore be left to the engineers taking the responsibility for the safety of their structures.

ROCK MASS DEFORMABILITY

The overall deformability of the rock mass is most important in analysing the stress in an arch dam and generally less important for gravity dams. Yielding abutments are of major concern for the development of cracks in an arch dam.

The deformation of a rock mass is governed by the deformability of the intact rock, its joints, and the extent to which the rock is fractured. With regard to the safety evaluation of existing dams, it is generally not the deformability itself of the rock mass that is important, but its possible change due to cyclic operation and time. If deformation measurements point to a deterioration of the rock which could potentially lead to sliding, then it is important to investigate the reasons why. Several hypotheses have to be checked, the most important of which are creep of the intact rock or of the joint filling, progressive fracturing, stress redistribution in the rock mass, changes in piezometric heads, or some combinations of these factors. When discussing methods of advanced deformation monitoring deep inside the rock, one has to remember these factors and their possible interplay.

ROCK MASS PERMEABILITY

In the context of sliding stability, the permeability of the rock foundation of large dams is crucial because it controls the buildup of water pressure along potential failure surfaces. Similar considerations apply to the stability of reservoir banks. As the permeability of the intact rock does not contribute markedly to the permeability of the rock mass in most cases, the percolation of water in the fracture network is decisive. Unfortunately, details about the nature of this network remain hidden from observation. It is safe to say that the degree of interconnection between fractures, the fracture aperture, and joint filling are the most important factors governing rock mass permeability. Grout curtains cause rapid pressure dissipation and a decrease of flow quantities, while drainage controls the intensity of the head in the rock. A functional drainage system is one of the most important factors in stability considerations.

When monitoring the behaviour of existing dams, the question which major discontinuities exhibit both change in aperture and in hydraulic head, and which discontinuities show only one or no such changes, is of utmost importance. Particular attention is paid to discontinuities which may kinematically serve as sliding surfaces.

Means of Monitoring Structural Behaviour

Monitoring is one of the main aspects of all dam safety programs. It supplements visual examination, because the lack of visible signs of an unexpected behaviour does not prove its non-existence. For all dams exceeding a given height or a certain impounding capacity, a so-called "basic program" is required by law. For example, in Switzerland, the minimum height for which such a basic program must be carried out is 10 metres, and the minimum impounding capacity is 50'000 cubic metres. The basic program (Biedermann, 1985) may include displacement measurements by surveying and by inverted pendulum and monitoring of uplift pressures. The nature of the instrumentation and the extent to which a dam should be instrumented is not outlined by law, but in some cases, the frequency of the readings and the review and reporting of the results is. For new dams, it is the responsibility of the designer to develop the instrumentation program, according to the size and type of the structure. Basic monitoring programs are carried out routinely in a continuous manner, and have two main objectives:

- to check or confirm the validity of the main design assumptions and to determine normal behaviour;
- to allow early recognition of deviations from normal behaviour.

"Additional monitoring" is required if, in a safety re-evaluation procedure, more detailed knowledge of the structural behaviour of the dam appears to be needed, or if the causes for an unexpected behaviour have to be elucidated. In this report, emphasis is placed on the discussion of the latter objectives which require not only additional installation of instruments, but also specific types of instrumentation techniques.

PHYSICAL QUANTITIES OF INTEREST

The selection of the physical quantities to be monitored depends on the nature of the anticipated process which could lead to sliding failure and on the capabilities of the available instruments. Sliding stability is controlled by the forces acting on the dam and by the available shear strength along the existing planes of weakness. Both the forces acting and the shear strength are quantities which may change, even if a constant reservoir level is considered. Disregarding, for now, the influence of potential earthquakes, or the effects of possible anchoring, a change in the forces may only be brought about by a variation in the distribution and the value of the piezometric head along the major discontinuities.

A reduction of the shear resistance may occur as a result of alterations of the material (joint filling, concrete at the base) or of small amounts of shear displacements. The piezometric head can vary in the course of time as a result of increasing permeability, i.e. a decrease of the pressure dissipation along flow paths takes place. Reasons for this may be fracture propagation, major leakage in the injection curtain, or ineffectiveness of drains, etc.

The basic problem of safety re-evaluations and that of finding the causes of an observed failure resides in the complex interrelationships which may prevail between the different factors listed above. In order to investigate details of such processes, the most important physical quantities to be measured will be the deformations and the piezometric heads. Because it is not known, in most cases, in which part of the rock mass or at which location of a discontinuity a detrimental process occurs, it is advantageous to measure the deformations and the piezometric heads using the principle of "linewise observation".

THE CONCEPT OF "LINEWISE OBSERVATION"

"Linewise observation" means measuring the distribution of a quantity along a line (Kovari and Amstad, 1983). The line can be given by the axis of a borehole or of a casing concreted into the structure. For example, one can obtain a full profile of the axial strain or of displacement vectors along a drill hole. This is in contrast to so called "point-wise observations," which only yield the quantities in some isolated points of the structure or of the rock.

Consider a straight line - referred to as measuring line - in a medium like rock mass or concrete. If the medium deforms, the line will also be deformed. The more we know about the deformations of the measuring line, the more we learn about the deformations of the medium in the vicinity of this line. How can the complete deformation of a straight line in three dimensions be geometrically described? Obviously, the continuous distribution of the three displacement vectors, u , v and w in a Cartesian system (x,y,z) along the line uniquely defines the line distortion. On the other hand, the distribution of the axial strain ϵ (shortening or extension), together with the curvatures κ_{xy} and κ_{xz} in two perpendicular planes, equally describe the deformations. Finally, the slopes α_{xy} and α_{xz} may also be used instead of the curvatures. From these equivalent ways of describing the complete deformation of a straight line, it follows that relationships between the different quantities exist. In fact, integrating the axial strain ϵ leads to the axial displacement u ; or the integration of the curvatures yields the corresponding slope angles which in turn, by means of a further integration, furnish the lateral displacements. Taking the x -axis in the direction of the borehole, it follows that the simple expressions below ensure geometrical compatibility:

$$\begin{aligned}
 u &= \int \epsilon \, dx & v &= \int \alpha_{xy} \, dx & w &= \int \alpha_{xz} \, dx \\
 \alpha_{xy} &= \int \kappa_{xy} \, dx & \alpha_{xz} &= \int \kappa_{xz} \, dx & \alpha_{yz} &= \int \kappa_{yz} \, dx .
 \end{aligned}$$

These relationships could also be written in a differential form expressing, for example, the axial strain ϵ as the derivative of the axial displacement u

$$\epsilon = \frac{du}{dx}, \quad \text{and} \quad \alpha_{xy} = \frac{dv}{dx}, \quad \text{etc.}$$

It is appropriate, therefore, to speak of *integrated quantities*, such as the displacement vector components, and of *differential ones*, like the axial strain and the curvature. The slope angles may be considered in both ways.

The question which may be raised is, the distribution of which quantities should be measured directly? The decision depends on two factors: first, on the type of the specific information expected from the monitoring, and secondly, on the feasibility of the available instrument techniques. From both points of view, preference should be given to the direct measurement of the distribution of differential quantities. A good example for linewise observations is the widely used inclinometer probe. This device is capable of measuring changes in inclination along a vertical borehole.

HIGH PRECISION DEFORMATION MEASUREMENTS

The achievement of consistent results with linewise observations calls for new types of instruments. Two basic criteria were applied in developing the measuring techniques:

- the portability of the instruments,
- the high precision of the readings.

The two conflicting requirements could be satisfied by the transformation of the continuous measuring line into a chain of well-defined reference points, the distance l between the points being constant (Fig. 3). Thus the problem of continuous deformation measurement is reduced to that observing the relative displacements of the adjacent reference point. For conditions of plane deformation, the following direct measured quantities are involved: the change of length Δl_i of a straight line, which may also be regarded as the strain ϵ on a base length l ; the change in slope angle $\Delta \alpha_i$, which also represents the curvature; and the slope angle α_i . For a straight line, the following relations, analogous to (1), are obtained between the direct and the derived quantities:



Fig. 3 Measuring the deformation of a straight line by means of a chain of reference points

$$u_n = \sum_0^n \Delta l_i + A$$

$$\alpha_n = \sum_0^n \Delta \alpha_i + B$$

$$v_n = 1 \sum_0^n \Delta \alpha_i + C$$

the displacement in the axial direction being designated by u and the lateral displacements by v .

For the determination of the three-dimensional displacement of a straight line, measurements are also carried out in a second plane, normal to the first one, and the relations above can be extended correspondingly. A, B and C are integration constants, the knowledge of which may be required for some problems. Often, either the values (u_0, v_0, α_0) at the mouth of the borehole or the values (u_n, v_n, α_n) at the bottom are known or measurable. We now consider different possibilities for a sliding device (Fig. 4). If only the change of distance Δl_i between two reference points is measured, we obtain the portable strain meter, the "Sliding Micrometer" (Kovari et al., 1979). For vertical measuring lines, an accelerometer can be added to monitor the slope angle α_i , in two perpendicular vertical planes, leading to the "Trivec" probe (Köppel et al., 1983). The name of the latter is intended to be a reminder of the fact that all three displacement components can be determined with this device. Finally, the so-called "Extensio-Deflectometer" probe consists of two members capable of slight rotation with respect to each other. It is designed to measure axial strain and the curvature along boreholes in any arbitrary direction. Here again, the distribution of all three displacement vectors can be calculated along the measuring line.

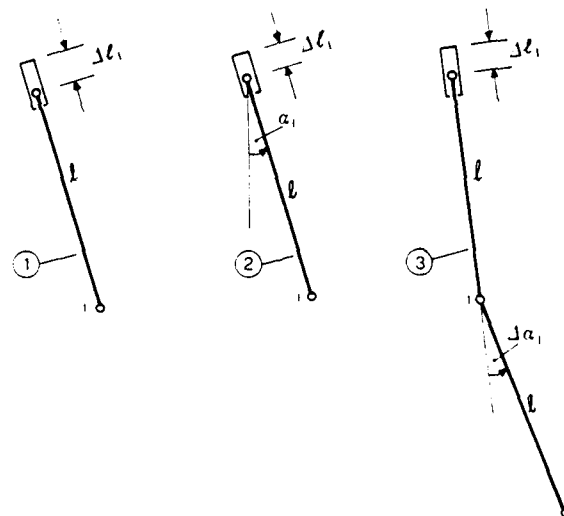


Fig. 4 Principles of portable borehole instruments for a chain of reference points

- 1) Sliding Micrometer
- 2) "Trivec"
- 3) "Extensio-deflectometer"

How should the reference points and the instrument ends be designed in order to obtain high precision in the readings? The principle applied here is that of a cone-sphere contact between the reference marks and the borehole probe. When a sphere is slightly pressed against a conical surface, the position of its center with respect to the cone is uniquely defined. Following this principle, the heads of the borehole probe have a spherical form and the reference marks are cone-shaped. This is well illustrated in Fig. 5, for the Sliding Micrometer. The plastic casing contains ring-shaped coupling elements which in turn carry the conical measuring marks. The whole casing is grouted into the borehole or progressively concreted into the dam during construction. In order to be able to move the instrument along the borehole from one measuring position to another, the conical and spherical parts are not complete. Turning the probe by $\pm 45^\circ$, brings it either into the measuring or into the sliding position, depending on its previous position (Fig. 4). The accuracy obtainable for setting the instrument in a measuring position is remarkably high. The relative displacement between two adjacent reference points in the axial direction can be obtained with an actual precision of $3 \mu\text{m}$ in the field. Considering the base length of 1.00 m of the Sliding Micrometer, this means that a strain determination with an accuracy of 3×10^{-6} can be achieved. Assuming a modulus of elasticity of the concrete or rock $E = 30\,000 \text{ N/mm}^2$, a change in stress can be determined with an accuracy of approx. 0.1 N/mm^2 ; this is sufficient for all practical purposes and illustrates well the high sensitivity of the device. The portability of the borehole probe permits its calibration at any time. In fact, a calibration frame made of invar steel is provided for checking the long-term stability of the LVDT sensor. Thus, any shift of the zero point can be compensated. The Sliding Micrometer and the Trivec are watertight up to a pressure of 15 bar. The Sliding Micrometer has been in use on a routine basis since 1978, and tens of thousands of meters of boreholes have already been instrumented and monitored in different countries. The longest borehole had a length of 90 m.

Experience using the Trivec, which yields both shear displacement and normal displacement along a borehole, also clearly meets the expectations (Amstad et al., 1987). To take a set of measurements with the Trivec (Fig. 6), beginning at the mouth of the borehole, the probe (a) is lowered in sliding position (b) and temporarily fixed into two adjacent measuring marks (c). There, a reading of the axial LVDT gauge and readings from the inclinometer in four positions are taken, initiated by a hand-held computer. The inclinometer sensor is therefore rotated by means of two micro-motors in the subsequent angular positions, 90 degrees apart from each other.

The results are sent to the hand-held computer. The probe is then lowered in a stepwise manner down the borehole, taking the five readings at every step in a similar manner.

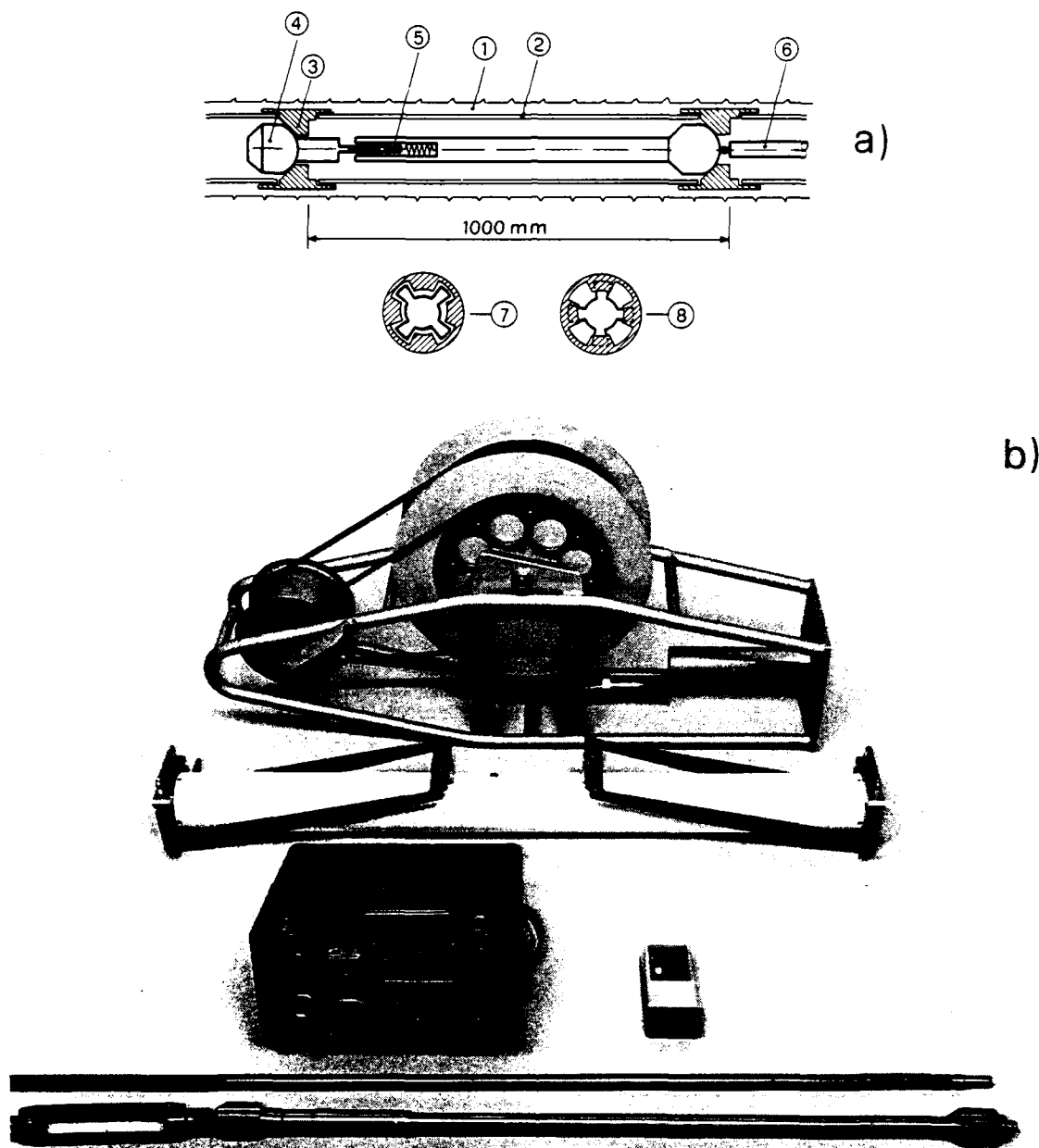


Fig. 5 Sliding Micrometer

a) Schematic view

1) Grouted borehole

2) Casing

3) Cone

4) Spherical head

5) Sensor

6) Operating Rod

7) Sliding position

8) Measuring position

b) Equipment with probe, installing rod, read-out unit, calibration frame and cable drum

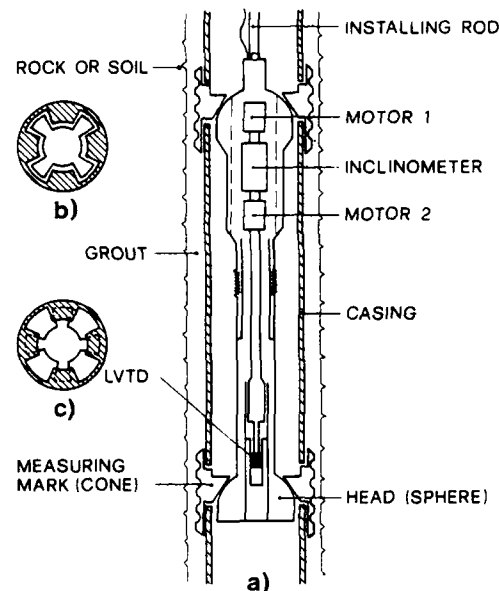


Fig. 6 Schematic view of the Trivec

- a) Instrument in measuring position in the borehole
- b) Sliding position
- c) Measuring position

After reaching the bottom of the measuring line, a repetition of all readings is made as the probe retraces its steps to the mouth of the borehole. This allows an immediate check, by the computer, of the accuracy in the field. Spurious readings can thus be detected at the site, and the repetition of readings can be made if necessary. A detailed description of the TRIVEC-system is given elsewhere (Köppel et al., 1983).

The Extenso-Deflectometer in its present form lacks a proper water insulation, restricting its application to dry holes. This device is therefore not yet available for wider use. It is discussed in this paper in order to illustrate the complete family of portable devices capable of linewise observation and based on the same cone-sphere setting principle. Furthermore, the Extenso-Deflectometer, as the most general type of such devices, offers great potential for practical applications. Let us now consider the difference between the information obtained from the Sliding Micrometer and that yielded by the Trivec (Fig. 7). If there is a differential movement along a joint resulting in the displacement vector $\Delta\delta$ (represented by $\overline{AA'}$), then the Sliding Micrometer will only provide the projection of $\Delta\delta$ on the measuring line, which is Δu . On the other hand, the Trivec is capable of yielding the vector $\Delta\delta$, i.e. the differential movements both parallel and normal to the joint surface ($\Delta\delta_n$ and $\Delta\delta_s$). In some cases, the additional information available from Trivec measurements are of great value for the understanding of the kinematics of a slide or the rock mass deformations.

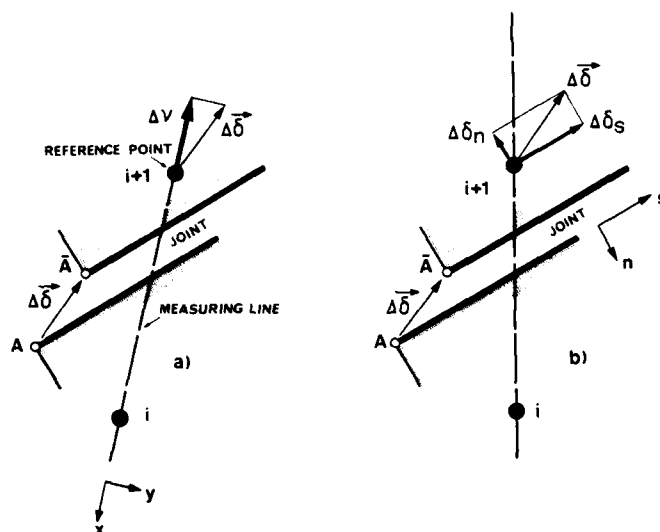


Fig. 7 Monitoring the relative displacements of a joint
 a) Sliding Micrometer with arbitrary direction providing the projection Δv of the displacement vector $\Delta\delta$ to the measuring line
 b) Trivec with vertical direction providing shear and normal displacements $\Delta\delta_s$ and $\Delta\delta_n$.

HIGH PRECISION WATER HEAD MEASUREMENTS

In the last decades, different techniques have been developed in order to obtain detailed fluid pressure distributions along boreholes. The Continuous Piezometer (Groupe de Travail du CFGB, 1970), with a single membrane along the entire length of a borehole, was developed in France, using a sliding probe to measure pressure at any location in the borehole. Patton developed the Modular Piezometer using a chain of packers and a sliding probe as a sensor (Patton, 1979).

The Piezodex system, described in the following, also involves a chain of packers and a sliding probe (Kovari and Köppel, 1987). The main difference between the two latter systems is the design of the packers and the principles of measurement. The modular packers use a tool that runs inside the casing and activates the packers individually. The Piezodex packers are interconnected by a continuous inflation line and filled with gas or a high-pressure, non-shrinking grout. The Modular Piezometer measures the fluid pressures directly, whereas the Piezodex probe uses a load cell without direct access to the fluid of which the pressure is to be measured. In the following, details of the Piezodex design, the accuracy of the instrument, and experience from field application are discussed.

The Piezodex System:

The following objectives regarding instrument performance were aimed at when developing this measuring system:

- great flexibility in selecting the number and length of measurement intervals, defined by a chain of packers;
- determination of the fluid pressure without any hydraulic connection between the sensor and the fluid in the measuring interval;
- minimizing the change in volume of the water in the measurement interval that could be brought about by a reading, i.e. avoiding affecting the pressure to be measured;
- using a single, sliding probe for readings in all the measurement intervals and in different boreholes;
- the possibility of calibrating and checking the functioning of the probe at any time and at any site;
- achieving a sensitivity of the readings of at least 0.02 % and an accuracy of the measurements of 0.1 % of the full selected measuring range.

The chain of packers: In order to define a series of measurement intervals (Fig. 8) along a borehole, a chain of packers is introduced and inflated using either nitrogen, a cement grout with special additives, or a two component resin. The nitrogen exhibits extremely low diffusion through the flexible membrane material. No leaks from packers or from connections was observed during the observation period of two years with a chain of packers having a total membrane length of 15 m with a total surface area in the inflated state of 4.7 m². A pressure of 15 bar was maintained during this period, using a compression cylinder containing nitrogen gas. The great advantage of using a gas is the possibility of recovering the chain of packers after completion of the measurements. One can also displace the packers, in order to change the measuring intervals in the borehole.

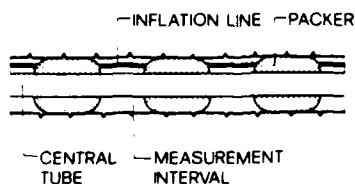


Fig. 8 Interconnected chain of packers defining individual measuring intervals

For long-term observations, packers filled with a special cement grout mixture are recommended. In order to prevent shrinkage, and to enhance volume increase during the curing of the cement, special additives are used. A high pressure is also applied (according to the anticipated fluid pressure difference) to the grout in the liquid state and during its setting. Considering the compressibility of the membrane of the packers, a large active pressure to the wall of the borehole can be maintained, even when the grout has solidified. Comprehensive laboratory test on grouted packers in a steel tube simulating the borehole confirmed the long-term water-sealing capacity of such packers, even for large differential water pressures. Any cement grout tends to bleed, to an extent that depends on the ratio of water to cement used. This means that in a horizontal or slightly inclined borehole, water accumulates at the top chord of the packer, and an empty space is left after the water is absorbed by the grout. As a result, the membrane is not pressed against the wall of the borehole on that top part. Therefore, a two component resin injected at high pressure must be used for boreholes inclined at less than 30° from the horizontal. Laboratory test have also proven this method of inflating the packers. Packers which use grouts of the types just mentioned can only be used in hard rock masses that show no noticeable creep as a result of the pressure applied on the packers to maintain the required sealing effects.

The location of measuring zones is selected according to the drill-core mapping of the rock supplemented, if needed, by remote video inspection or other joint exploration techniques. Packers may thus be placed at irregular intervals, depending on the position of the main fractures intersecting the borehole. In the case of extensive jointing, a regular arrangement of the packers is proposed, with the option of displacing the whole chain of gas-inflated packers in the following observation period. There are no specific constraints as to the number of monitoring zones, except for the geometry of the equipment (length of the packers and connections). In order to obtain a reliable seal, a minimum length of 1.00 m is suggested for the packers. The shortest length of a measuring interval is 0.5 m. The casing of the Piezodex is watertight, so the probe can be operated under dry conditions. This prevents any conductivity along the casing in the borehole.

The measuring system consists of two main parts: the pressure transmitter cells and the sliding Piezodex probe (Fig. 9). The continuously assembled, watertight tube carrying the packers is fitted with pressure transmitters that merely transmit the fluid pressure to the force sensor in the probe. The fluid acts on an extremely thin elastic membrane on the surface of the pressure transmitter; this membrane rests on a piston which transmits the force to the sensor in the probe. This assembly (Fig. 10) is located in a casing that also acts as connection element for the various tube sections (Fig. 11). When the probe is brought into measuring position, the pressure transmitter is lifted by 0.2 mm, and the force F required to counter the water load is measured (Fig. 12).

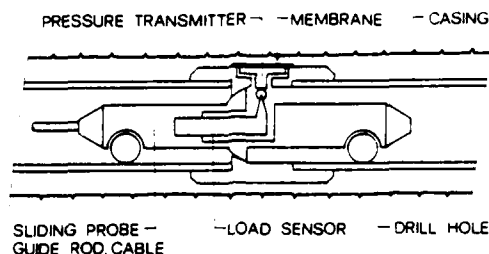


Fig. 9 The Piezodex probe in measuring position slightly lifting the built-in pressure transmitter which is loaded by water pressure

This force is proportional to the water pressure p and the surface area of the piston. The piston is supported by ball bearings, in order to avoid any sliding friction. By selecting pistons with different sizes, i.e. with different areas A , different values of the sensitivity and of the measuring range can be obtained for the same load sensor in the probe. Pressure transmitters for maximum pressures of 5, 10, and 29 bar have so far been applied. Two different types of transmitters can be placed in one measuring interval, to ensure a high accuracy of the reading and a larger measuring range. The second main part of the measuring system is the probe itself (Fig. 9), which is a kind of torpedo that can be moved along the tube and driven up to the pressure transmitters on any of the measuring intervals. The probe is brought into measuring position using the same principle as for the Sliding Micrometer (Kovari et al., 1979). The stops in the casing on which the probe sits have a conical shape, and the seating surface of the probe is spherical. The readings thus obtained have a reproducibility in the range of less than 0.01 mm. Here again, the stops in the casing and the seat of the probe are only part of a cone and a sphere, respectively. The probe can be turned by 45° to be brought into either the measuring or the sliding position, and moved along the tube to any of the pressure transmitters. At the heart of the probe is a load sensor having the form of a cantilever and fitted with strain gauges. The unique features of this sensor are its high resolution, linearity and insensitivity to changes in temperature or in humidity, due to an advanced coating technology. The accuracy in terms of force is better than 0.02 N for a measuring range of 0 - 50 N.

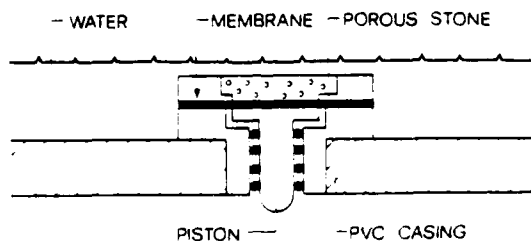


Fig. 10 Schematic view of the pressure transmitter

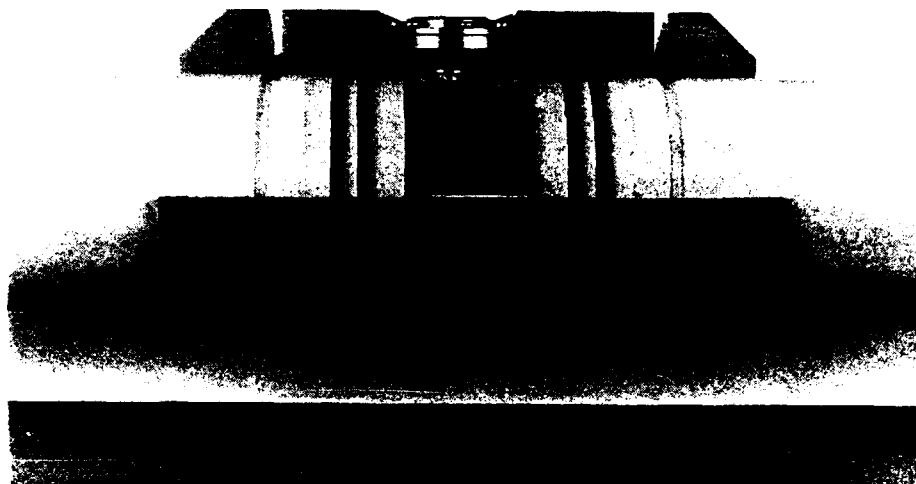


Fig. 11 The pressure transmitter fixed in the coupling element of the casing (cut open for better view)

The equipment, as it is used in vertical or steeply inclined boreholes, is shown in Fig. 13. In such boreholes, no guiding rod is necessary to rotate the probe through 45° , into or out of the measuring position. For this purpose, the probe is provided with a servomotor. In boreholes with an orientation that does not permit the probe to slide under the simple action of gravity, the guiding rod is used to turn and move the device. To perform a set of readings along a borehole, one starts with the measuring interval next to the mouth of the borehole and proceeds step by step until the last interval along the hole is reached. When retrieving the probe, the readings are repeated, to check the first values and to improve their reliability.

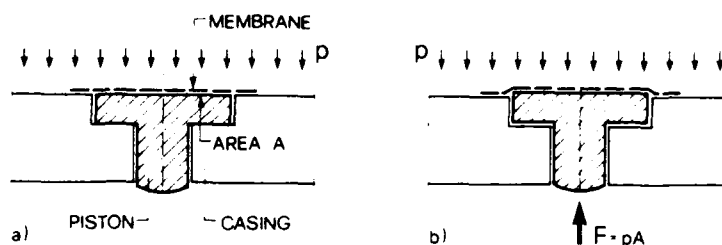


Fig. 12 The pressure transmitter with membrane
 a) in normal position acted upon by the fluid pressure p
 b) slightly lifted by the probe in reading position, also acted upon by the measured force F

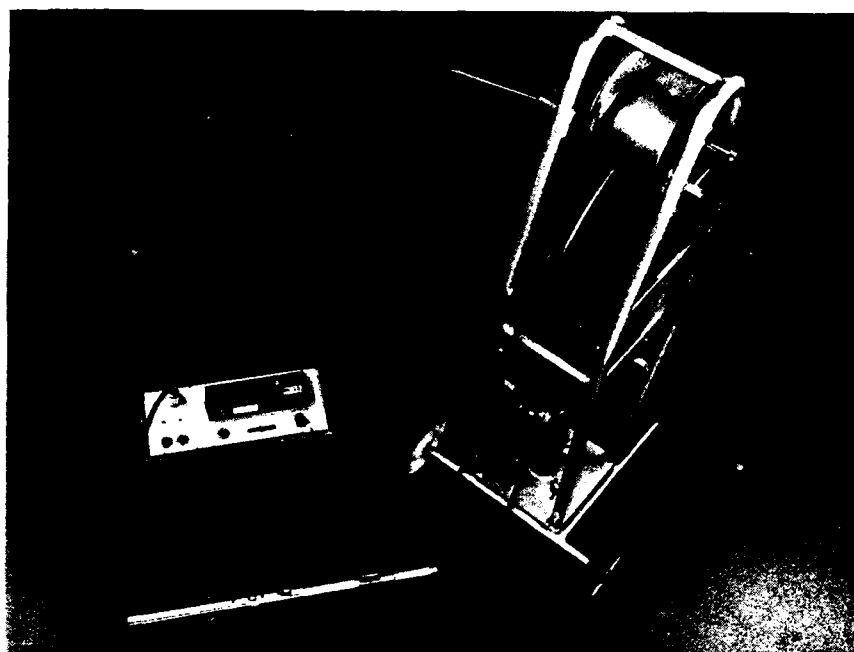


Fig. 13 The Piezodex probe with cable reel and readout unit

Calibration of the probe: The load cell, together with the readout unit should be calibrated prior to and after a series of readings. A simple, portable calibration apparatus using different weights has been designed for this purpose (Fig. 14). Fig. 15 shows the probe resting on the calibration support in a horizontal position, loaded with one weight unit. The calibration allows the detection of a possible deviation from linearity or any sign of hysteresis.

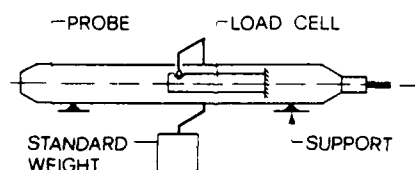


Fig. 14 Calibration of the load cell using standard weights

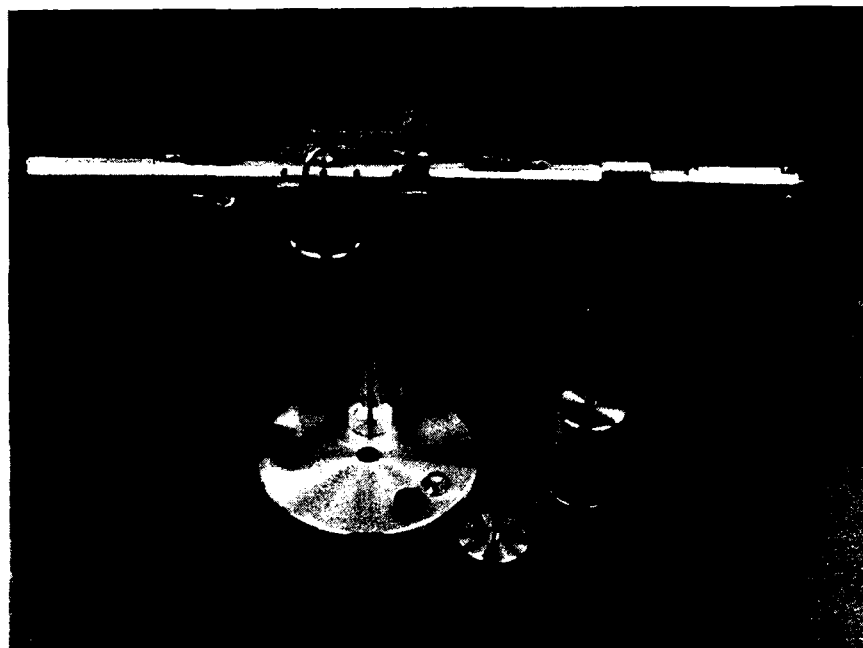


Fig. 15 The probe on the calibration support, loaded by a weight unit

INTERPRETATION OF MEASUREMENTS

All the information about the structure of the rock mass must be considered for interpreting the results of field measurements. Only in doing this can one fully understand the mechanism that might lead to a decrease in safety against sliding of a particular dam or rock embankment. Linewise observations are, as mentioned earlier, particularly useful in this regard. Especially to be noted is the potential value of Trivec measurements.

Simple sliding mechanisms - representing the basic types for stability calculations - and the expected results are represented schematically in Figs. 16-18. The rigid-body sliding of a rock mass on a slope results in a single peak of the strain values ϵ and α_{xz} (Fig. 16a). The horizontal displacement components v and the displacement vector δ are evenly distributed. Further, parallel sliding planes in the rock mass (Fig. 16b) manifest themselves as additional peaks in the differential values ϵ and α_{xy} . Differences in velocity between masses 1 and 2 can be derived from jumps in the distribution of v and δ .

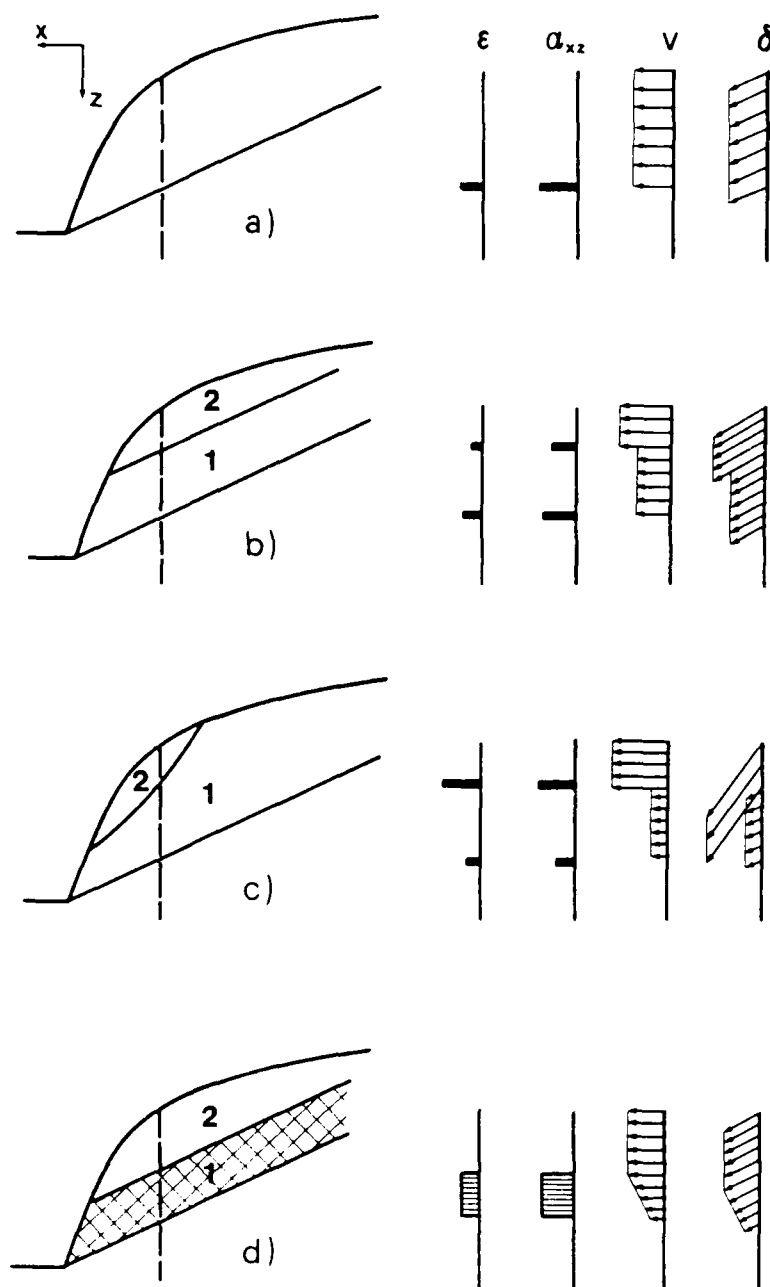


Fig. 16 Measured values and displacement vectors for simple plane failure

- a) Sliding on a single plane
- b) Sliding on two parallel planes
- c) Sliding on two arbitrarily oriented planes
- d) Creeping in zone 1

Fig. 16c shows the sliding mechanism for two superposed rock masses of different shapes and whose sliding surfaces are not parallel. Mass 2 slides over mass 1 on a curved surface, while the latter slides on an inclined plane. The distribution of ϵ , α_{xy} , and v obtained from the Trivec measurements are similar to those in Fig. 16b. The distribution of the resultant vector δ , however, is quite different, in that not only different values, but also distinct directions of motion can be observed for masses 1 and 2. This fundamental value (δ) can not be obtained from e.g. inclinometer measurements.

The case illustrated in Fig. 16d is that of a thick, creeping layer (1) which is responsible for the displacement of the overlying mass (2). For the purpose of a schematic representation, a constant shearing strain resulting in linearly increasing displacements from the bottom to the top was assumed for mass 1. Horizontal displacements v and the resultant displacement vector δ do not change in mass 2.

Fig. 17 is a schematic representation of a mass consisting of parts 1 and 2 sliding on a polygonal surface. Two boreholes, starting at points A and D, in which Trivec measurements were taken, are indicated. If it can be assumed, once more, that the rock masses move as rigid bodies, then we can expect two peaks in the distribution of ϵ and α in the upper borehole, while only one peak should show up in the lower one. The graph for ϵ was left out of Fig. 17. The sign for α at point B, i.e. at the intersection of the borehole and the internal sliding surfaces should be noted. In this case as well, assuming polygonal sliding surfaces, it is the resultant displacement vectors δ , with their different directions, that yield the key to understanding the sliding mechanism.

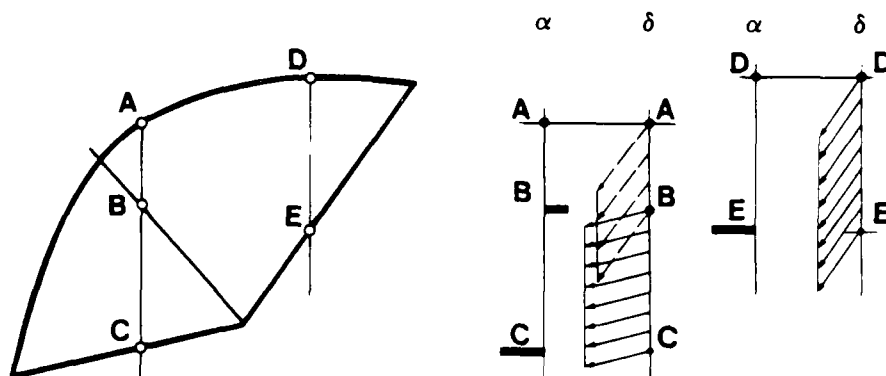


Fig. 17 Measured values and displacement vectors for sliding on a polygonal surface

For the sake of completeness, we also present briefly the idealized measured results obtained with the Trivec for a wedge-shaped sliding surface. Fig. 18 shows two measuring lines, each traversing two sliding surfaces. In this case, the resultant displacements δ are not parallel to the sliding planes, but rather to the intersection s of the planes.

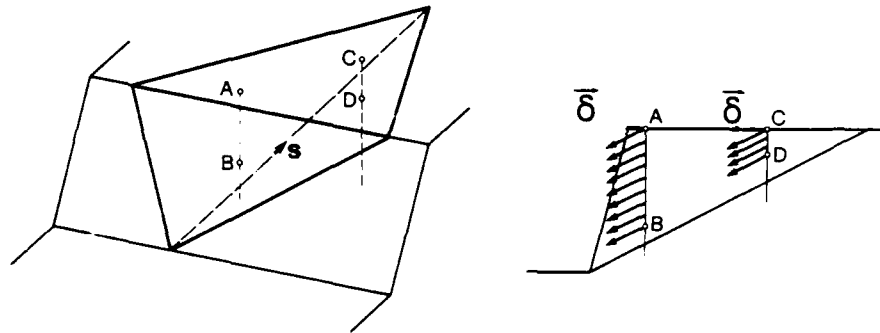


Fig. 18 Displacement vectors for a wedge type failure

Stability Analysis

INTRODUCTION

The main methods for solving slope stability problems are *limit analysis*, with its main representative, the limit equilibrium method, and *complete analysis* including the range of elasticity and constrained plastic flow, e.g. the finite element method. Although most promising from a theoretical point of view, complete analyses have not been widely accepted in practice for slope stability investigations because of several impediments. For example, the required formulation of a stress versus strain relation is more intricate than the formulation of a strength criterion. Furthermore, an interpretation of the resulting distribution of stresses and strains is much more demanding than the discussion of a scalar value such as the factor of safety.

Limit analysis investigates the collapse load without having to follow the step-by-step procedure of elasto-plastic analyses. Generally speaking, three conditions are needed for a valid solution in mechanics, namely the stress-equilibrium equations, the stress-strain relations and the compatibility equations relating strain and displacement. If some of these conditions are disregarded (in order to minimize the computational effort), lower or upper bound solutions may be obtained. Lower bound solutions rely on stress equilibrium and yield criteria, but they do not consider kinematics. They give rise to safety factors which are too low, i.e. less or equal to the exact solution. Upper bound solutions rely on kinematically admissible velocity fields or failure modes and the so-called flow rule, and lead to safety factors which are too high, i.e. greater or equal to the exact solution.

Following the engineering practice, we limit ourselves to the *limit equilibrium method*, which relies on assuming a simplified mode of failure and formulating overall equations of static equilibrium. Although the limit equilibrium method utilizes the basic philosophy of upper-bound solutions, it does not meet the precise requirements of the upper or lower bound method (Chen, 1975). However, with a suitable choice of the failure mode, the method may yield an answer approaching the correct solution.

For the limit equilibrium method, the rock is idealized as a rigid body or an assembly of rigid bodies. Rotation and lifting off is disregarded in the present work, i.e. only sliding, which must occur along plane surfaces, is considered. However, the necessary conditions to exclude rotation, i.e. toppling, form an integral part of the mechanical derivations. A factor of safety is defined, which provides a measure of the distance from the limit equilibrium. This definition has given rise to extensive discussions in the literature. Following the usual concept in civil engineering, the factor of safety F is defined as the ratio of the shear strength τ_{\max} to the effective shear stress τ acting in a failure surface (Bishop, 1955),

$$F = \frac{\tau_{\max}}{\tau} \quad (1)$$

Safety is thus measured as a reserve of strength. Substitution of the shear strength according to Coulomb for the effective normal stress σ , the angle of friction ϕ , and the cohesion c , leads to

$$\tau = \sigma \frac{\tan \phi}{F} + \frac{c}{F}$$

i.e. F may also be interpreted, as was already mentioned above, as a number by which both shear parameters (ϕ and c) must be divided in order to reach limit equilibrium (Taylor, 1948).

It has been suggested (Rocha, 1978) to apply different numbers - so called partial safety factors - for the friction coefficient (F_ϕ) and the cohesion (F_c) respectively, that is

$$\tau = \frac{1}{F} \left(\sigma \tan \phi + \frac{F}{F_c} c \right)$$

Such a procedure usually simply involves a more or less arbitrary reduction of the cohesion with respect to the friction coefficient while using basically the same safety concept.

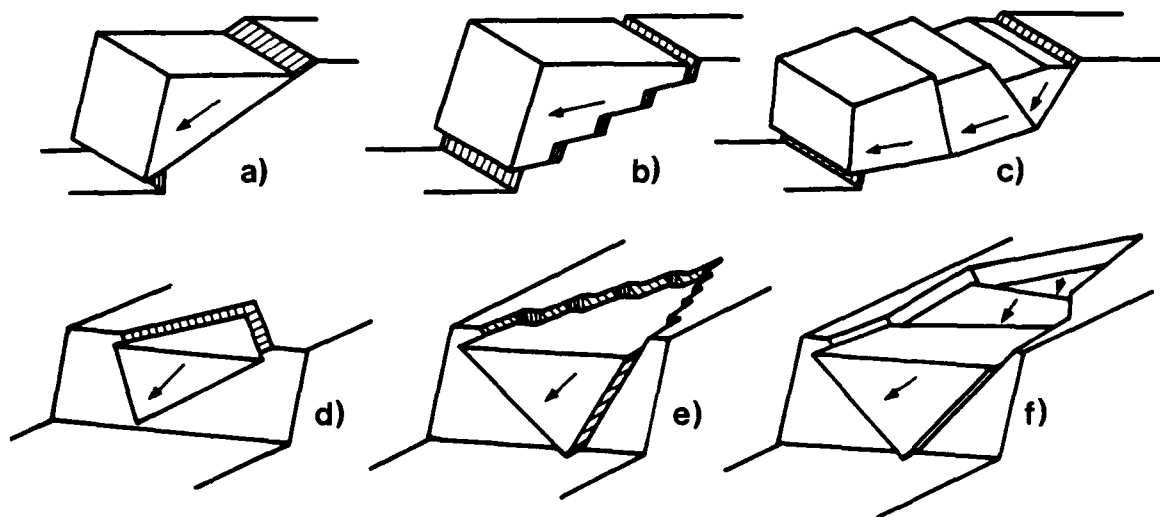


Fig. 19 Failure mechanisms for sliding of a rock mass

Another definition of the factor of safety, which has been widely applied, is based on a qualitative grouping of the forces acting on the sliding mass (Burmister, 1946). F is expressed as the ratio of the so-called resisting forces to the so-called driving forces. This definition is mechanically incorrect and may lead to contradictory results (Kovari and Fritz, 1978). It should therefore not be used.

In the following, a mathematical formalism is presented which comprises both simple applicability, to allow extensive parameter analyses, and a unified treatment of the basic sliding mechanisms observed in rock slopes (Fig. 19). The most important factors which influence the stability of a rock slope are taken into account.

SIMPLE PLANE FAILURE

Simple plane failure involves sliding on a single plane. A vertical section through a potential sliding mass is shown in Fig. 20. The geometry of the slope is defined by the area A of the sliding plane, its dip angle α and, indirectly, by the weight W of the sliding mass. Introducing the weight W of the sliding body explicitly means that no further geometrical data are required. Thus, the detailed specifications of the shape of the sliding body do not enter into the calculations.

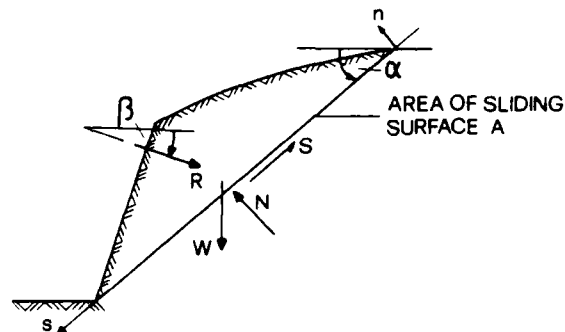


Fig. 20 Simple plane failure

The resultant of the external forces R (e.g. anchor force) dips with an angle β to the horizontal. The reaction on the sliding plane is composed of a shear force S and a normal force N . For this system, relationships may be formulated for force equilibrium in the n and s directions,

$$N = R \sin(\alpha + \beta) + W \cos \alpha \quad (2)$$

$$S = -R \cos(\alpha + \beta) + W \sin \alpha, \quad (3)$$

for the maximum shear resistance S_{\max} along the sliding plane according to Coulomb,

$$S_{\max} = N \tan \phi + cA, \quad (4)$$

and the factor of safety, analogous to (1)

$$F = \frac{S_{\max}}{|S|} \quad (5)$$

Because lifting off is not considered, the normal reaction should be positive i.e.

$$N > 0 \quad (6a)$$

Combination of relations (2) to (5) yields the sought-for basic formulae which are the key to the unified treatment of slope stability problems, namely for the factor of safety F

$$F = |q_1 (\tan\phi + \frac{cA}{W} q_2)| \quad (6b)$$

$$\text{where } q_1 = \frac{\cos\alpha + (R/W) \sin(\alpha + \beta)}{\sin\alpha - (R/W) \cos(\alpha + \beta)}$$

$$q_2 = \frac{1}{\cos\alpha + (R/W) \sin(\alpha + \beta)}$$

or, rearranged for the resultant R ,

$$R = k_1 \left(1 - \frac{cA}{W + p^W} k_2 \right) W \quad (6c)$$

$$\text{where } k_1 = \frac{F \sin\alpha - \cos\alpha \tan\alpha}{F \cos(\alpha + \beta) + \sin(\alpha + \beta) \tan\phi}$$

$$k_2 = \frac{1}{F \sin\alpha - \cos\alpha \tan\phi}$$

It may be observed that the coefficients k_1 , k_2 and q_1 , q_2 are independent of the cohesion and the shape of the sliding mass. Therefore, the cohesion c appears explicitly in the expressions for F and R , which allows a simple and immediate estimate of its influence. Furthermore, if no other external forces are acting besides the anchor force, equation (6c) may be used directly as a design formula for the anchor force.

To facilitate the evaluation of the anchor force, especially in the field, the coefficients k_1 and k_2 have been assembled in design charts (Kovari and Fritz, 1976). Fig. 21 shows such a chart for k_1 for an angle $\beta = 40^\circ$ and a factor of safety of 1.5. For a vanishing cohesion, k_1 represents directly the anchor force normalized by the weight of the rock mass. The corresponding chart in Fig. 22 for the coefficient k_2 holds also for a factor of safety of 1.5, whilst it is independent of β . The curves for k_2 demonstrate the great influence of the cohesion c .

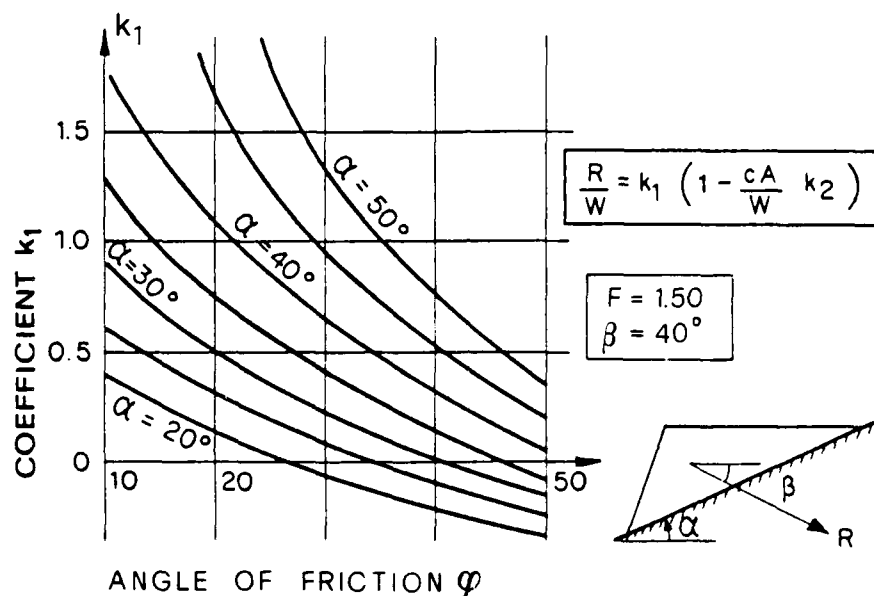


Fig. 21 Coefficient k_1 for $\beta=40^\circ$ and factor of safety $F=1.5$

It is worth mentioning that formulas (6) also hold, as will be shown afterwards, for the three dimensional problem of a wedge-type failure. Furthermore, they may easily be extended (Kovari and Fritz, 1984) to apply to other, most frequently encountered problems in engineering practice. The corresponding forms of the basic equations (6) are listed in Table 1. Case (A) refers to a natural slope with or without the presence of an uplift force. Thus, the formula for F serves for a safety assessment or for a back analysis of the strength parameters assuming $F = 1$. It will also reveal the effect of a drainage of the slope. Case (B) provides a solution for the determination of the anchor force R required to stabilise a slope or to determine its influence on safety. The general case (D) may be especially interesting in the context of foundation of large dams or bridges and also as the basis for the stability analysis involving polygonal failure surfaces.

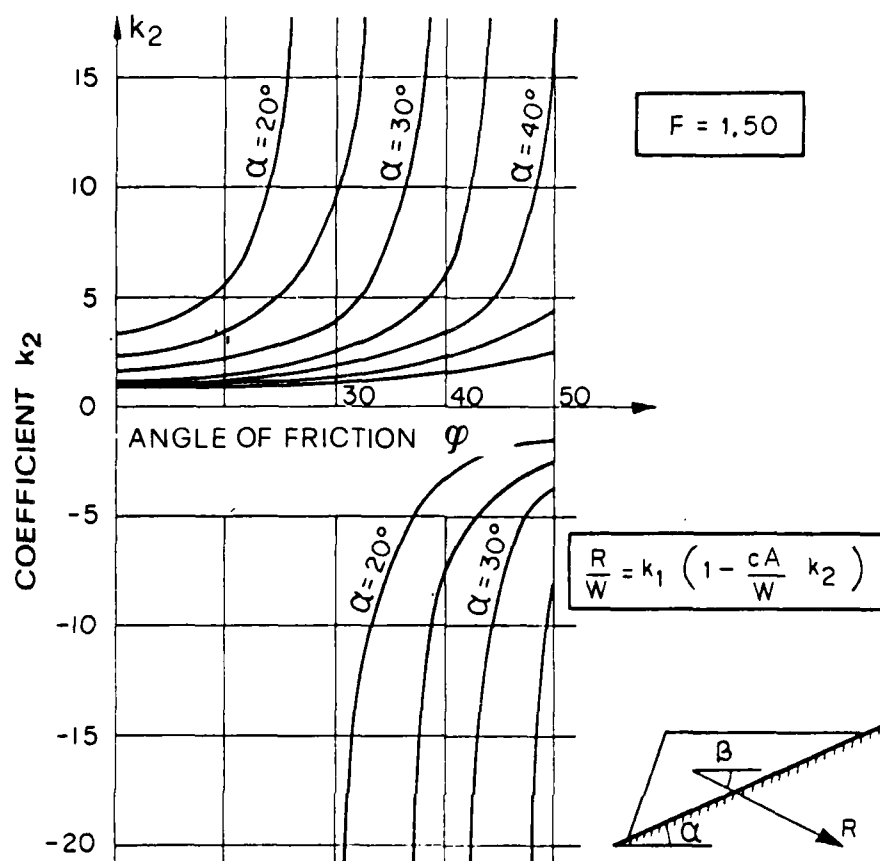


Fig. 22 Coefficient k_2 for a factor of safety of $F=1.5$

Up to this point, the third equilibrium condition (equilibrium of moments) has not yet been formulated, i.e. the factor of safety for simple plane failure may be determined without considering moment equilibrium. However, moment equilibrium may be formulated to ensure that sliding, and not toppling, is the relevant mode of failure.

With the geometrical definitions of Fig. 23, moment equilibrium may be formulated for the intersection of N with the sliding plane in the form

$$W (s_A - s_N) - R (s_N - s_R) = 0 \quad (7a)$$

or rearranged for the distance s_N of the point of action of N

$$s_N = \frac{Ws_A + Rs_R}{W + R} \quad (7b)$$





CASE	FORMULAE	UPLIFT FORCE		COEFFICIENTS	
		$U = 0$	$U \neq 0$	q	k
(A) natural slope $R = 0$ $P = 0$	 $F = \left q_1 \left(\tan \phi + \frac{cA}{W} q_2 \right) \right $	\leftarrow		$q_1 = \frac{1}{\sin \alpha}$ $q_2 = \frac{1}{\cos \alpha}$	
		\rightarrow			
(B) anchored slope $P = 0$	 $F = \left q_1 \left(\tan \phi + \frac{cA}{W} q_2 \right) \right $ $R = k_1 \left(1 - \frac{cA}{W} k_2 \right) W$	\leftarrow		$q_1 = \frac{\cos \alpha + \frac{R}{W} \sin(\alpha + \beta)}{\sin \alpha - \frac{R}{W} \cos(\alpha + \beta)}$ $q_2 = \frac{1}{\cos \alpha + \frac{R}{W} \sin(\alpha + \beta)}$	
		\rightarrow			
(C) water in tensile crack $P = 0$ $U_T \neq 0$	 $F = \left q_1 \left(\tan \phi + \frac{cA}{W + U_T \tan \beta} q_2 \right) \right $ $R = k_1 \left(1 - \frac{cA}{W + U_T \tan \beta} k_2 \right) (W + U_T \tan \beta)$ $+ \frac{U_T}{\cos \beta}$	\leftarrow		$q_1 = \frac{\cos \alpha + \frac{R}{W + U_T \tan \beta} \sin(\alpha + \beta)}{\sin \alpha - \frac{R}{W + U_T \tan \beta} \cos(\alpha + \beta)}$ $q_2 = \frac{1}{\cos \alpha + \frac{R}{W + U_T \tan \beta} \sin(\alpha + \beta)}$	$k_1 = \frac{f \sin \alpha - \cos \alpha \tan \phi}{f \cos(\alpha + \beta) + \sin(\alpha + \beta) \tan \phi}$ $k_2 = \frac{1}{f \sin \alpha - \cos \alpha \tan \phi}$ with $f = \text{sign}(F, S)$
		\rightarrow			
(D) General Case	 $F = \left q_1 \left(\tan \phi + \frac{cA}{W + P^W} q_2 \right) \right $ $R = k_1 \left(1 - \frac{cA}{W + P^W} k_2 \right) (W + P^W) - P^T$	\leftarrow		$q_1 = \frac{\cos \alpha + \frac{R + P^T}{W + P^W} \sin(\alpha + \beta)}{\sin \alpha - \frac{R + P^T}{W + P^W} \cos(\alpha + \beta)}$ $q_2 = \frac{1}{\cos \alpha + \frac{R + P^T}{W + P^W} \sin(\alpha + \beta)}$	

Table 1: Various forms of the basic formula for special cases of simple plane failure

Toppling may not occur if N acts within the sliding plane, i.e.

$$0 \leq s_N = \frac{Ws_A + Rs_R}{W + R} \leq s_A.$$

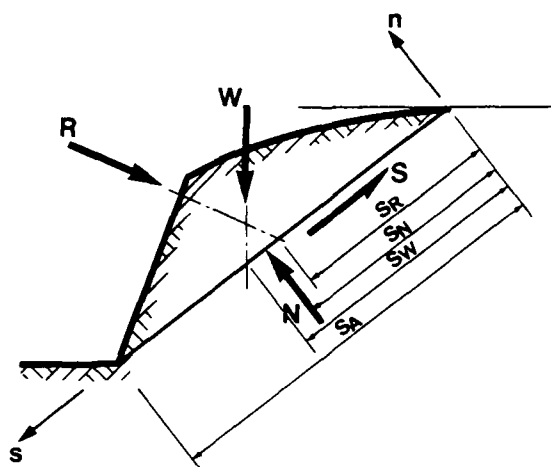


Fig. 23 Geometry of simple plane failure

Equation (8) is sufficient to prevent toppling. However, strictly speaking, it is not sufficient to satisfy all derivations made earlier. If tensile stresses in the sliding surface are activated, condition (4) for the shear strength according to Coulomb theoretically no longer holds. However, for a first approach, this recognition may be neglected. If we imagine a natural sliding surface with its rough undulations and its asperities, this approach does not seem unrealistic.

SIMPLE WEDGE FAILURE

It will be shown here how the three-dimensional problem of a wedge sliding on two planes can be reduced to the simple plane failure mode handled above.

A cartesian coordinate system (s, n, h) is defined as follows (Fig. 24): the s -axis is determined by the line of intersection of the two planes, the n -axis lies in the vertical plane through s , and the h -axis is horizontal. The geometry of the wedge is essentially determined by the areas A_I and A_{II} of the sliding planes, the dip angle α_s and dip direction ψ_s of the line of intersection, the angles ω_I and ω_{II} between the n -axis and the sliding planes and, indirectly, by the weight W of the sliding mass. The determination of the angles from the measured dip angles and dip azimuths of the sliding planes is simply a matter of geometry.

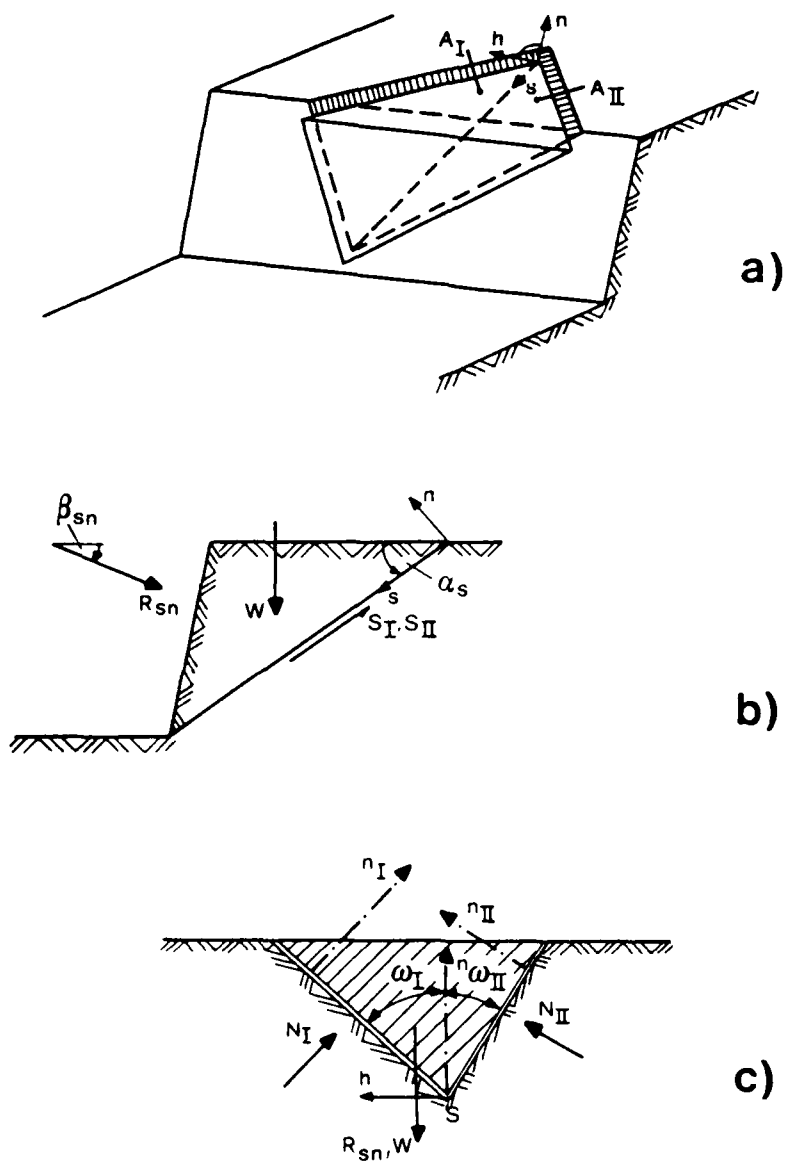


Fig. 24 Isometric view and sections of a simple wedge
 a) Isometric view
 b) Vertical plane through line of intersection of the sliding surfaces
 c) Plane normal to line of intersection

The forces acting are divided into three groups:

- self-weight W ;
- reactions (here two normal forces N_I and N_{II} and two shear forces S_I and S_{II});
- the resultant R of the external forces.

Similarly to the case of one sliding plane, the basic relationships may be formulated for

- the equilibrium conditions;
- the definition of the factor of safety;
- Coulomb's law of friction for shear resistance along the sliding surface.

Initially, it will be assumed, for the sake of simplicity, that the resultant $R_{s,n}$ lies parallel to the vertical plane (s,n) through the intersection line, and further, that the same friction angle applies to both planes. The combination of the five conditions with the help of elementary algebraic operations yields (Kovari and Fritz, 1978) the following basic equations for wedge problems, namely the conditions to prevent uplift

$$\begin{aligned} N_I &> 0 \\ N_{II} &> 0, \end{aligned} \quad (9a)$$

the factor of safety

$$F = |q_1^* (\tan\phi + \frac{c_I A_I + c_{II} A_{II}}{W} q_2^*)| \quad (9b)$$

$$\text{where } q_1^* = \frac{\cos\alpha_s + (R_{sn}/W) \sin(\alpha_s + \beta_{sn})}{\sin\alpha_s - (R_{sn}/W) \cos(\alpha_s + \beta_{sn})}$$

$$q_2^* = \frac{1}{\cos\alpha_s + (R_{sn}/W) \sin(\alpha_s + \beta_{sn})}$$

and, rearranging the resultant $R_{s,n}$

$$R_{sn} = k_1^* \left(1 - \frac{c_I A_I + c_{II} A_{II}}{W} k_2^* \right) W \quad (9c)$$

$$\text{where } k_1^* = \frac{F \sin \alpha_S - \cos \alpha_S \tan \phi^*}{F \cos(\alpha_S + \beta_{SN}) + \sin(\alpha_S + \beta_{SN}) \tan \phi^*}$$

$$k_2^* = \frac{1}{F \sin \alpha_S - \cos \alpha_S \tan \phi^*}$$

$$\tan \phi^* = \frac{\cos \omega_I + \cos \omega_{II}}{\sin(\omega_I + \omega_{II})} \tan \phi = \lambda \tan \phi .$$

One immediately recognizes the correspondence of the formulae with that for simple plane failure and the conditions for an analogy:

- instead of the slope angle α of the single failure surface, the dip angle α_S of the line of intersection of the two failure surfaces is employed,
- instead of the friction angle ϕ , an apparent angle ϕ^* is used,
- instead of the product cA , the sum $c_I A_I + c_{II} A_{II}$ must be considered.

Thanks to this analogy, the same graphs may be used for the coefficients k_1^* and k_2^* as for k_1 and k_2 (Fig. 21 and 22). The inclination α_S of the intersection line and the factor λ for determining the angle ϕ^* may be determined by means of a pocket calculator or a personal computer, or they may even be depicted from a table. As an illustrative example Table 2 may serve: for discrete values of the dip angles α_I , α_{II} of the sliding planes and the difference $\Delta\psi$ of their strike orientation, the table provides sets of α_S (upper values) and λ (lower values).

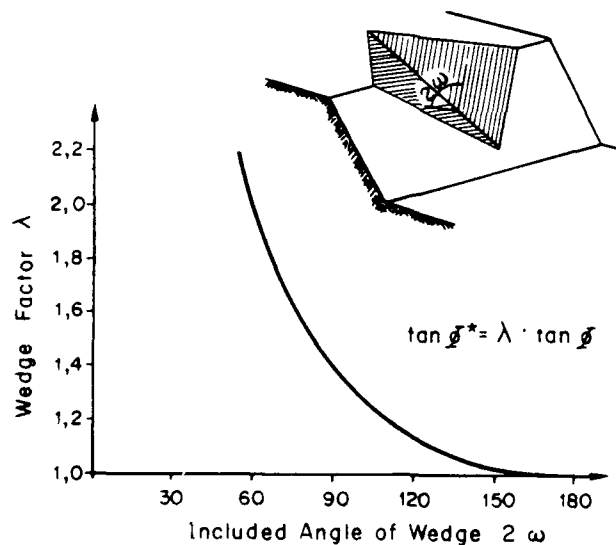


Fig. 25 Wedge coefficient λ for a symmetrical wedge as a function of the included angle of wedge

The coefficient

$$\lambda = \frac{\tan \phi^*}{\tan \phi}$$

reflects the apparent increase of the friction angle due to the wedge effect. White spaces in the table indicate sliding on one plane only, i.e. when the wedge type of failure is not relevant. Fig. 25 displays the coefficient λ as a function of the included wedge angle 2ω for a symmetric wedge ($\omega = \omega_I = \omega_{II}$).

Relations (9) may again be easily extended for the most important problems encountered in practice. Table 3 shows some special cases for illustrating purposes.

Dip 1st plane	Dip 2nd plane	DIFFERENCE OF DIP ORIENTATION												
		150	140	130	120	110	100	90	80	70	60	50	40	30
45	45	14.5	18.9	22.9	26.6	29.8	32.7	35.3	37.5	39.3	40.9	42.2	43.2	44.0
		1.37	1.34	1.30	1.26	1.23	1.19	1.15	1.12	1.09	1.07	1.05	1.03	1.02
	50	15.7	20.4	24.7	28.5	31.9	34.9	27.5	39.6	41.5	43.0	44.1	44.8	
		1.42	1.39	1.34	1.30	1.25	1.21	1.17	1.13	1.10	1.07	1.04	1.02	
55	55	16.9	21.9	26.4	30.3	33.8	36.8	39.3	41.4	43.1	44.3	44.9		
		1.48	1.43	1.38	1.33	1.28	1.23	1.18	1.13	1.09	1.05	1.02		
	60	18.1	23.3	28.0	32.1	35.6	38.5	40.9	42.8	44.1	44.9			
		1.54	1.49	1.42	1.36	1.30	1.24	1.18	1.13	1.08	1.03			
50	50	17.1	22.2	26.7	30.8	34.4	37.5	40.1	42.4	44.3	45.9	47.2	48.2	49.0
		1.49	1.44	1.39	1.34	1.28	1.24	1.19	1.15	1.11	1.08	1.06	1.04	1.02
	55	18.6	23.9	28.7	33.0	36.6	39.8	42.5	44.7	46.5	48.0	49.1	49.8	
		1.55	1.50	1.44	1.37	1.31	1.26	1.28	1.16	1.12	1.08	1.05	1.02	
55	55	20.3	26.0	31.1	35.5	39.3	42.6	45.3	47.6	49.5	51.0	52.3	53.3	54.1
		1.64	1.57	1.49	1.42	1.35	1.28	1.23	1.18	1.13	1.10	1.07	1.04	1.02
	60	22.1	28.2	33.5	38.0	41.9	45.1	47.8	50.0	51.8	53.2	54.3	54.9	
		1.72	1.64	1.55	1.46	1.38	1.31	1.24	1.18	1.13	1.09	1.05	1.02	
60	60	24.1	31.6	36.2	40.9	44.8	48.1	50.8	53.0	54.8	56.3	57.5	58.4	59.1
		1.83	1.72	1.61	1.51	1.42	1.34	1.26	1.20	1.15	1.11	1.07	1.05	1.03

Upper values: Dip angle α_s

Lower values: Wedge coefficient λ

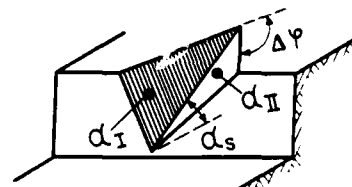


Table 2: Inclination of intersection line α_s and wedge coefficient λ for different wedge geometries

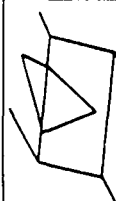



CASE	FORMULAE	$\tan \phi^*$	COEFFICIENTS	$k_{1,2}^*$
 (A) symmetric natural slope $R^h, p^h=0$	$F = \frac{1}{2} \left[\tan \phi^* + \frac{c(A_1 + A_{II})}{W} - q_2^* \right]$	$\frac{1}{\sin \alpha} \tan \phi$	$q_1^* = \frac{1}{\sin \alpha}$ $q_2^* = \frac{1}{\cos \alpha}$	$k_{1,2}^*$
 (B) symmetric slope	$F = \frac{1}{2} \left[\tan \phi^* + \frac{c(A_1 + A_{II})}{W + p^v} - q_2^* \right]$ $R_{sn} = k_1^* \left(1 - \frac{c(A_1 + A_{II})}{W + p^v} k_2^* \right) - (W + p^v) - p^v \sin \alpha$	$\frac{1}{\sin \alpha} \tan \phi$	$q_1^* = \frac{R_{sn} + p^v}{\cos \alpha_s} \frac{R_{sn} + p^v}{W + p^v} \sin(\alpha_s + \delta_{sn})$ $q_2^* = \frac{R_{sn} + p^v}{\sin \alpha_s} \frac{R_{sn} + p^v}{W + p^v} \sin(\alpha_s + \delta_{sn})$	$k_1^* = \frac{f \sin \alpha_s - \cos \alpha_s \tan \phi^*}{k_1^* f \cos(\alpha_s + \delta_{sn}) + \sin(\alpha_s + \delta_{sn}) \tan \phi^*}$ $k_2^* = \frac{1}{f \sin \alpha_s - \cos \alpha_s \tan \phi^*}$ with $f = \text{sign}(P, S_I + S_{II})$
 (C) symmetric loading $R^h, p^h=0$	$F = \frac{1}{2} \left[\tan \phi^* + \frac{c(A_1 + A_{II})}{W + p^v} - q_2^* \right]$ $R_{sn} = k_1^* \left(1 - \frac{c(A_1 + A_{II})}{W + p^v} k_2^* \right) - (W + p^v) - p^v \sin \alpha$	$\frac{\cos \omega_{II} \tan \phi_I + \cos \omega_I \tan \phi_{II}}{\sin(\omega_I + \omega_{II})}$	$q_1^* = \frac{R_{sn} + p^v}{\cos \alpha_s} \frac{R_{sn} + p^v}{W + p^v} \sin(\alpha_s + \delta_{sn})$ $q_2^* = \frac{R_{sn} + p^v}{\sin \alpha_s} \frac{R_{sn} + p^v}{W + p^v} \sin(\alpha_s + \delta_{sn})$	$k_{1,2}^*$
 (D) general case	$F = \frac{1}{2} \left[\tan \phi^* + \frac{c(A_1 + A_{II})}{W + p^v} - q_2^* \right]$ $R_{sn} = k_1^* \left(1 - \frac{c(A_1 + A_{II})}{W + p^v} k_2^* \right) - (W + p^v) - p^v \sin \alpha - k_1^* k_2^* (R^h + p^h)$ with $k_1^* = \frac{\sin \omega_{II} \tan \phi_I - \sin \omega_I \tan \phi_{II}}{\sin(\omega_I + \omega_{II})}$	$\frac{\cos \omega_{II} \tan \phi_I + \cos \omega_I \tan \phi_{II}}{\sin(\omega_I + \omega_{II})}$	$q_1^* = \frac{R_{sn} + p^v}{\cos \alpha_s} \frac{R_{sn} + p^v}{W + p^v} \sin(\alpha_s + \delta_{sn})$ $q_2^* = \frac{R_{sn} + p^v}{\sin \alpha_s} \frac{R_{sn} + p^v}{W + p^v} \sin(\alpha_s + \delta_{sn})$	$k_{1,2}^*$

Table 3: Various forms of the basic formula for special cases of simple wedge failure

POLYGONAL PLANE FAILURE

It is known from experience that sliding, due to the nature of the discontinuities in rock, frequently takes place on polygonally shaped surfaces. For such cases, Janbu (1954) and Morgenstern and Price (1965) have suggested practical methods of computation, whereby the endangered earth or rock mass is divided up into vertical strips or slices. The computational procedure is based on certain assumptions regarding the distribution and direction of internal contact forces. Kinematical admissibility of the velocity field is not considered, i.e. no internal failure is considered. This leads to unrealistic failure modes. Sultan and Seed (1967) were possibly the first in drawing the attention to the fact that sliding on a polygonal surface consisting of two planes is kinematically only possible if failure occurs also in the slope material itself.

Based on this recognition, the method developed here assumes that sliding on "external" polygonal sliding planes (Fig. 26) provokes internal shear planes to develop, which start from the intersection lines of the external sliding planes (Kovari and Fritz, 1978). Thus, sliding of a mass on n external sliding planes is accompanied by $n-1$ internal shear planes. The directions of the internal shear planes may be chosen from structural investigations of the potential sliding mass. For highly jointed rock, the directions may be found by satisfying the condition of having the minimum factor of safety for the whole system.

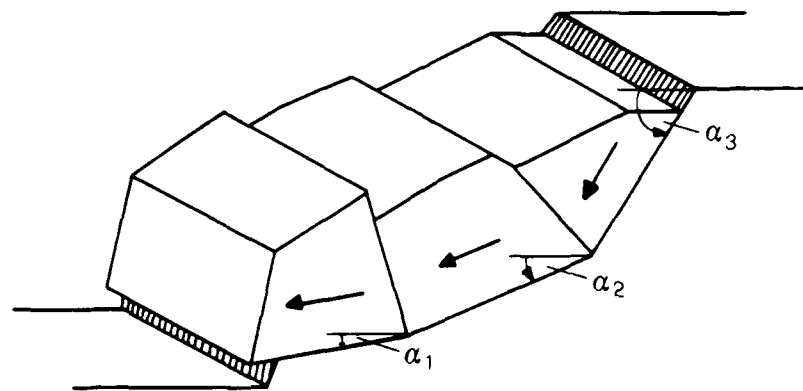


Fig. 26 Polygonal plane failure

The mathematical treatment is based on applying the basic formula (6c) to each of the n rock blocks and formulating the failure criterion (4) together with (5) for each of the $n-1$ internal shear planes. The same factor of safety is assumed in all external sliding planes and internal shear planes. This seems most reasonable because the safety factor for all surfaces must reach unity at the moment of slip. This has been discussed extensively elsewhere (Kovari and Fritz, 1978).

Considering that a contact force with two unknown components is acting on each internal shear plane and that, additionally, the overall safety factor also has to be determined, the number of unknowns amounts to $2(n-1) + 1 = 2n - 1$. The total number of relationships mentioned above also amounts to $n + (n-1) = 2n - 1$. Therefore, a unique solution of the problem exists for a given geometry, loading and strength. It is pointed out that the values of the shear parameters may be different for each of the external or internal sliding surfaces.

Fig. 27 shows the i -th block of a rock mass which fails in a polygonal manner. The notation for such a block is essentially the same as for the simple plane case, only an index characterising the i -th block is added. The unknown forces, R_i are here the contact forces between the individual blocks. Given load quantities are introduced by the force P_i . Parameters applying to the internal shear planes are designated by a bar. Therefore uplift forces acting in the external sliding surface are designated by U_i , whereas those acting in the internal shear planes by \bar{U}_i . For each of the n blocks, the extended equation (6c) (c.f. the general case in Table 1) becomes

$$R_i = k_{1i} \left(1 - \frac{c_i A_i}{W_i + P_i^W + R_{i-1}^W} k_{2i} \right) (W_i + P_i^W + R_{i-1}^W) - (P_i^R + R_{i-1}^R) \quad (10)$$

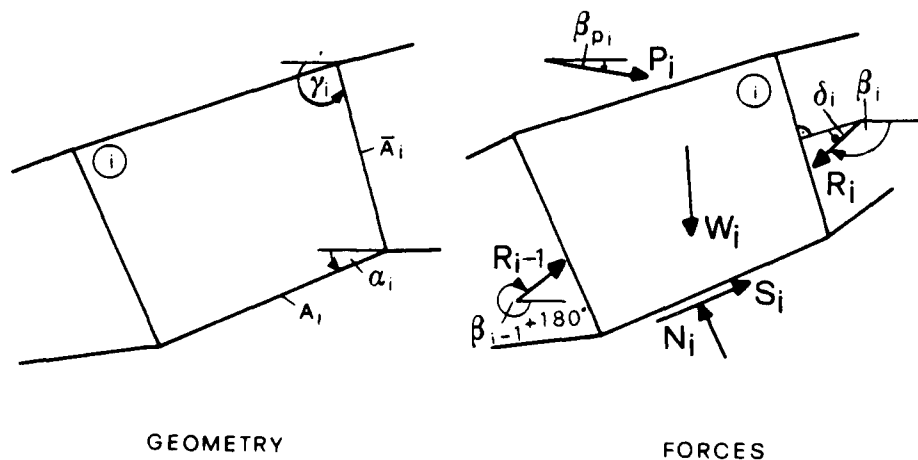


Fig. 27 Block i of a rock mass on a polygonal sliding surface

$$\begin{aligned}
 \text{where } k_{1i} &= \frac{F_i \sin \alpha_i - \cos \alpha_i \tan \phi_i}{F_i \cos(\alpha_i + \beta_i) + \sin(\alpha_i + \beta_i) \tan \phi_i} \\
 k_{2i} &= \frac{1}{F_i \sin \alpha_i - \cos \alpha_i \tan \phi_i} \\
 c_i &= c_i - (U_i/A_i) \tan \phi_i \\
 F_i &= F \operatorname{sign}(1, S_i),
 \end{aligned}$$

where the subscripts w and r denote the resolution of the corresponding force in direction of W_i and R_i . Expression (4) for the maximum shear resistance according to Coulomb and (5) for the factor of safety may furthermore be formulated for each of the $n-1$ internal shear planes in the form

$$\begin{aligned}
 \bar{S}_{\max i} &= (\bar{N}_i - \bar{U}_i) \tan \bar{\phi}_i + \bar{c}_i \bar{A}_i \\
 \bar{S}_{\max i} \\
 F &= \frac{\bar{S}_{\max i}}{|\bar{S}_i|}
 \end{aligned}$$

$$\begin{aligned}
 \text{where } \bar{N}_i &= R_i \cos \delta_i \\
 \bar{S}_i &= R_i \sin \delta_i.
 \end{aligned}$$

Combining these two expressions yields an implicit expression for the inclination β_i of the contact force R_i

$$\begin{aligned}
 \beta_i &= -(\delta_i + \gamma_i + 90^\circ) \\
 \tan \delta_i &= \frac{1}{\bar{F}_i} \left(\tan \bar{\phi}_i + \frac{\bar{c}_i \bar{A}_i}{R_i \cos \delta_i} \right) \quad (11)
 \end{aligned}$$

$$\begin{aligned}
 \text{where } \bar{F}_i &= F \operatorname{sign}(1, \bar{S}_i) \\
 \bar{c}_i &= \bar{c}_i - (\bar{U}_i/\bar{A}_i) \tan \bar{\phi}_i.
 \end{aligned}$$

Equations (10) and (11) form a system of non-linear equations for the unknown contact forces and their directions as well as for the value of the overall factor of safety. In practice, only the system (10) of degree n is solved directly, equations (11) being satisfied by means of an iterative procedure (Kovari and Fritz, 1978). This solution method proved to be very simple and inexpensive. Problems with regard to mathematical convergency have not been encountered.

The solution must be checked for kinematical admissibility: the sliding directions must be compatible (all shear forces in the external sliding planes should have the same sign) and contact between the blocks must be guaranteed (the components of the effective reactions normal to the corresponding failure plane should all be positive). If one of these conditions is not fulfilled, another sliding mechanism will be relevant, e.g. sliding of some lower blocks only.

It is worth mentioning that, for the polygonal slope stability problem, the factor of safety and all forces involved may be determined without considering equilibrium for moments. Equilibrium conditions for moments are formulated by some authors aiming at determining the location of the reactions and the internal contact forces. With this knowledge, it would be possible to check the physical admissibility of the solution, e.g. if the reactions are acting within the corresponding failure planes. However, because only n moment conditions are available, but $n+1$ unknown locations of the reactions exist, $n-1$ assumptions must be made for a proper solution. Since innumerable possibilities for these assumptions exist, it always seems possible to find a physically admissible solution (Sarma, 1979), although one can not be certain whether it is a relevant one (Chen and Morgenstern, 1981).

Equilibrium of moments may be formulated for a limiting case with the aim to determine potential toppling. Toppling of a polygonal slope is controlled by the ability of the toe block to topple: the starting failure mechanism of the slope will only be toppling if the toe block topples, i.e. if the normal reaction N_1 of the toe block lies outside the corresponding sliding plane (Fig. 27). The only unknown value for the toe block is the point of action of the contact force R_1 . In the sense of a limiting formulation, R_1 may be assumed to act at the upper end of the internal shear plane. If toppling can be excluded for this limiting case, only sliding stability of the slope must be considered. In the opposite case, toppling may or may not be relevant. Further information may not be obtained by the present approach without introducing arbitrary and therefore questionable assumptions.

Case Histories

KÖLNBREIN ARCH DAM

The Kölnbrein arch dam belongs to the Malta pumped storage scheme in the south part of the Austrian Alps, at an elevation of 1700 m (Fig. 28). The capacity of the reservoir is $200 \times 10^6 \text{ m}^3$, the dam has a maximum height of 200 m, and a crown length of 620 m, which well illustrates the great importance of this structure. The foundation rock on the right bank consists of massive granite gneiss, whereas on the left bank, gneisses with fine shistosity occur. The central part is crossed by shistose gneiss. The dam was completed in 1977, but the filling of the reservoir had started already a year before. During the subsequent service period, an unexpected behaviour of the dam was observed, manifesting itself as an excessive loss of water, the formation of cracks in the concrete, but also in the development of displacements differing considerably from design predictions. This gave rise to a comprehensive program of investigations including strain distribution measurements using the Sliding Micrometer. The total length of the drill holes instrumented for this purpose reached approximately 1,000 m in 1984. Other types of instrumentation have also seen a considerable increase in the course of years, thus reflecting the difficulties in identifying the exact causes of the detrimental behaviour. In the following, the strain distribution along some selected boreholes due to changes in water head will be presented and specific features discussed. Fig. 28 shows the location of blocks 17 and 18 in the central part of the dam, this area responding particularly sensitively to the reservoir fluctuations.

Results of Measurements at Block 18:

The measuring lines M2 and M3 were aimed at detecting both cracks in the concrete structure and active joints in the foundation rock. The horizontal borehole M1 (Fig. 29) illustrates the effect of reservoir filling to its maximum water level at the elevation of 1,902 m on the strains. The reference readings were taken at a water level of 1,720 m corresponding to the scour outlet. The sharp peaks in the strain curve reveal at first glance that two cracks in the concrete intersect the measuring line and a major fissure separates the upstream heel of the dam from the rock. Such occurrences have often been the subject of discussions. It is also clear from this figure that the rock traversed by the borehole must also be heavily cracked. The complete separation of the dam from the rock in the horizontal direction is manifested by the drop of strain to zero in the concrete. Looking at the curve pertaining to a reservoir head at 1,840 m, one may realize that a pre-existing crack in the concrete closes and another crack only opens at higher reservoir heads. From the two curves it is also evident that a shift in strain distribution in the direction of extension strains takes place as the reservoir head increases.

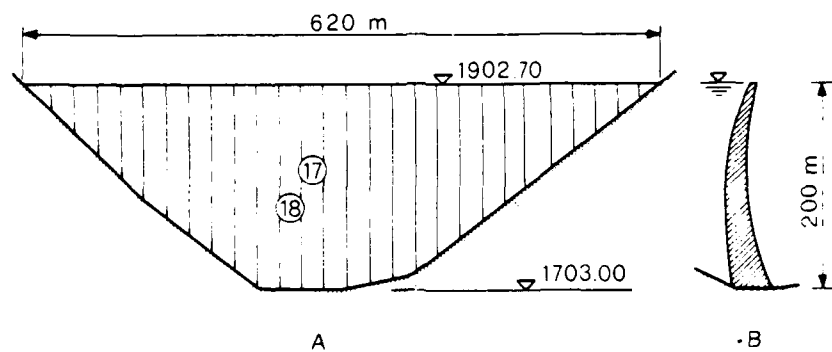
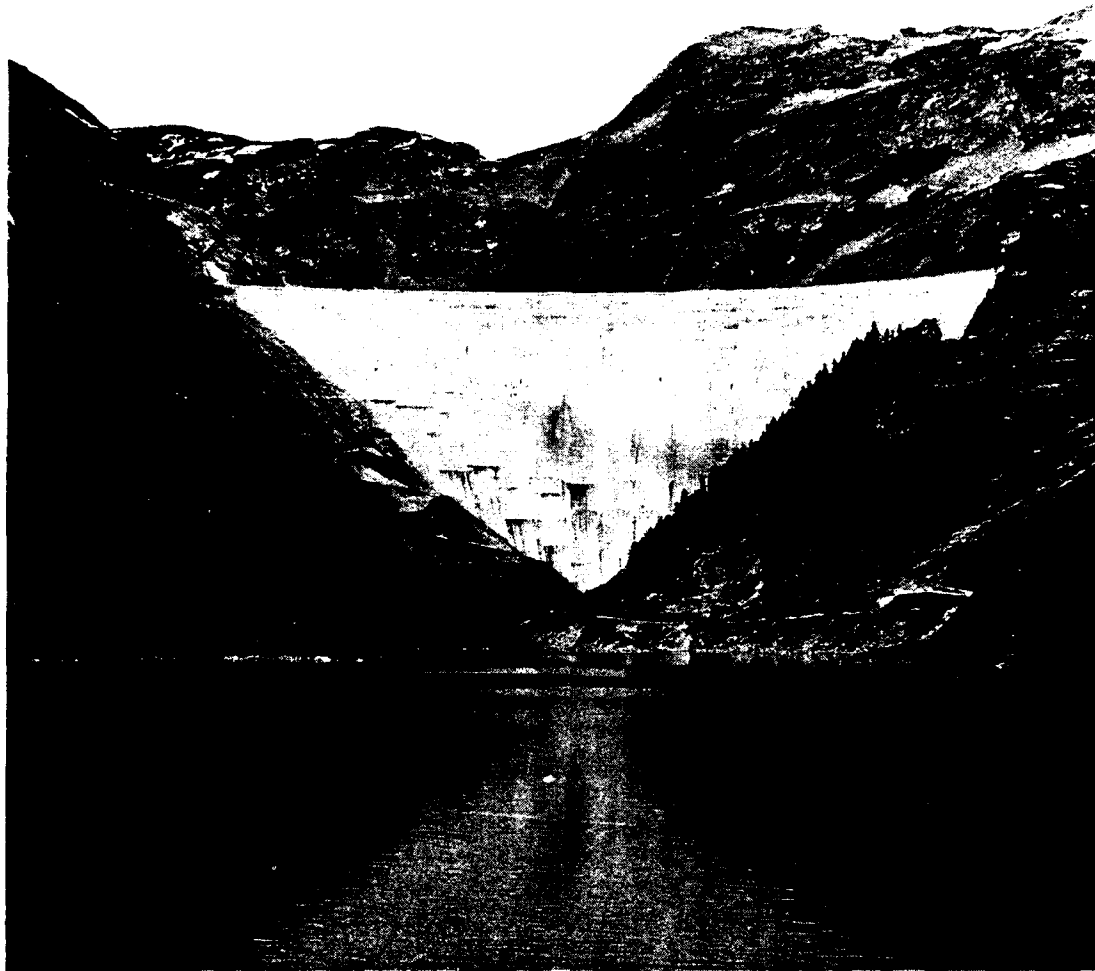


Fig. 28 Kölnbrein Arch Dam
A. Front view
B. Cross section

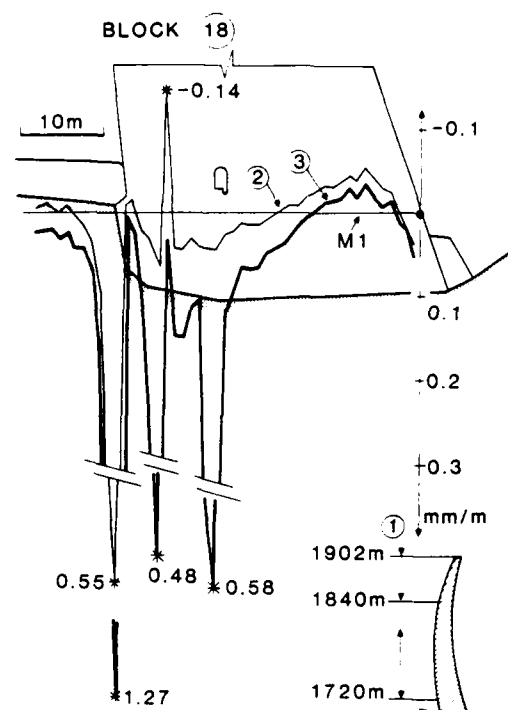


Fig. 29 Strain development due to reservoir filling

M1. Measuring line

1. Extension strain

2. Water level at 1'840 m

3. Maximum water level

In Fig. 30, the effect of decreasing water level on the strain development both in the concrete and the foundation rock along the inclined measuring line M2 is illustrated. Three curves are represented, demonstrating the relative importance of the water level on the closure of fissures. Two major cracks in the concrete are revealed by the curves. One of them daylights the downstream surface of the dam and its closing and opening could be independently monitored by a simple LVDT-gauge. The results of the Sliding Micrometer measurements and the direct crack monitoring on the downstream concrete surface were found to agree well, taking into consideration the distance of two meters between the bore-hole and the surface gauge. A further peak of the strain curves occurs at the downstream toe of the dam, leading to a significant drop of strain on both sides of the peak. Apart from the peaks and the drops, the "average" strains in the concrete and the adjacent rock mass exhibit similar values that indicate a deformability modulus of the rock close to that of the concrete. The strain distribution in the foundation rock indicates areas with alternating rock quality.

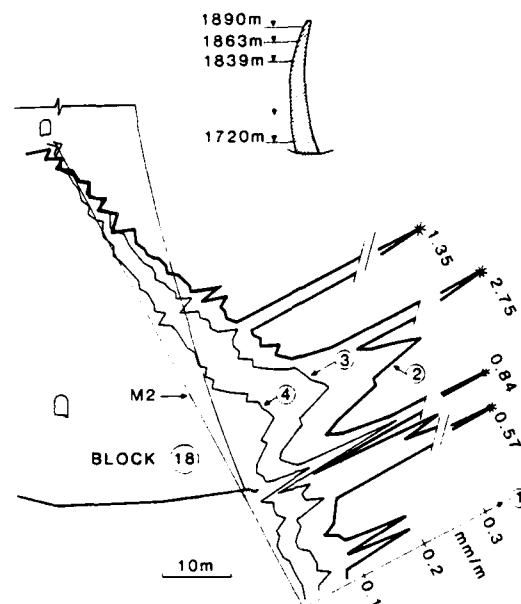


Fig. 30 Strain development due to fall in water level

M2. Measuring line

1. Extension strain
2. Water level at 1'720 m
3. Water level at 1'839 m
4. Water level at 1'863

Results of Measurements at Block 17:

At this block, a connecting adit running perpendicular to the dam axis exists, connecting the bottom outlet with the main drainage gallery. From this adit, a vertical and two inclined boreholes were drilled in order to explore the deformation behaviour of the concrete and the rock in the area of the downstream toe (Fig. 31 to Fig. 33). The reference readings of the strain curves were taken again at a water level of 1,720 m corresponding to the scour outlet. From the diagrams in Fig. 31 and Fig. 33, the presence of a weak rock of approximately 2 m thickness immediately becomes apparent. On the other hand, the measuring line M4 in Fig. 32 exhibits no peak at its intersection with the concrete rock interface. A minor peak exists two meters below the concrete. Either the weak zone in the rock does not extend to the line M4 or the strain is such that its component in the direction of this measuring line becomes for some other reason small. In order to obtain the principal strains and their directions in two dimensions, three measuring lines intersecting each other at the same point would be needed. The uneven distribution of strain, Fig. 31 to Fig. 33 - apart from the above-mentioned sharp peaks - reflects again the discontinuous and nonhomogenous character of the rock mass.

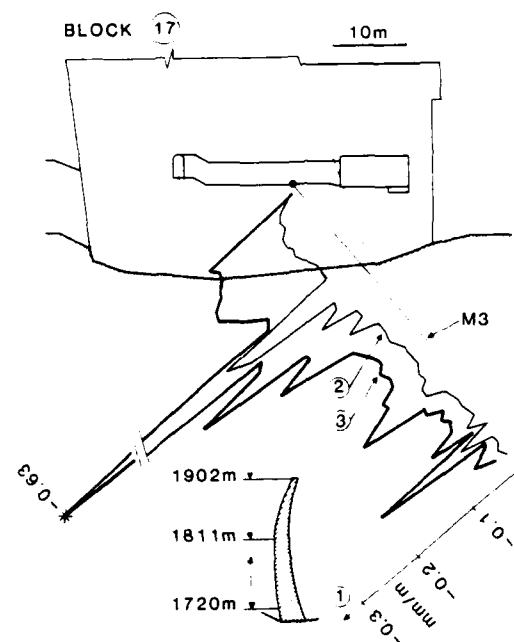


Fig. 31 Strain development due to reservoir filling
 M3. Measuring line
 1. Compression strain
 2. Water level at 1'811 m
 3. Maximum water level

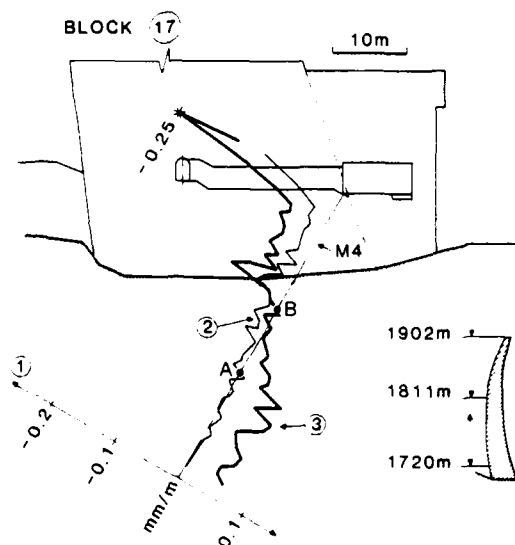


Fig. 32 Strain development due to reservoir filling
 M4. Measuring line
 1. Compression strain
 2. Water level at 1'811 m
 3. Maximum water level

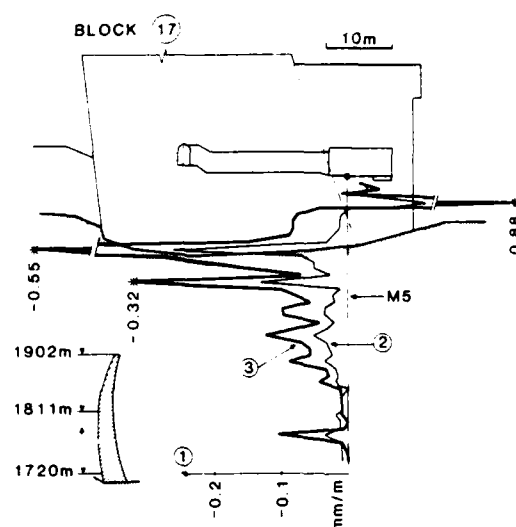


Fig. 33 Strain development due to reservoir filling

- M5. Measuring line
- 1. Compression strain
- 2. Water level at 1'811 m
- 3. Maximum water level

From the curves in Fig. 31, it can be inferred that the modulus of elasticity of the concrete and that of the rock (disregarding the presence of the weak zone) are very similar. The borehole for the measuring line M5 in Fig. 33 was drilled from the concrete structure of the bottom outlet traversing the dam in a short stretch and extending 32 m deep into the rock. The peak near the borehole mouth indicates a crack in the bottom outlet with an opening of 0.88 mm at full reservoir. The continuation of this crack into the dam concrete could be detected by the measuring line M4 (Fig. 32) which shows its direction. The most interesting finding from Fig. 32 is the considerable increase of extension strains with increasing reservoir head. The curve corresponding to a reservoir filling of 50% suggests a compression zone in the rock extending to the point A. Below this point, the strains are negligibly small. At full reservoir, however, the end of the compression zone seems to shift to point B, near the base. Furthermore, a considerable tension zone is indicated, with no perceivable stress dissipation until the end of the borehole. Thus, increasing water level not only affects the magnitude of deformations but it confirms a major redistribution of the stress in the foundation rock. Considering the results of all three measuring lines M3, M4, and M5 (Figs. 31 to 33), the conclusion emerges that a reduction of the compression zone in the rock beneath the upstream toe occurs when raising the reservoir.

This in turn might be caused by two effects occurring simultaneously (Fig. 34):

- decrease of the load transfer surface at the base;
- and change in the inclination of the dam thrust with an increased ratio of the shear force to the normal force.

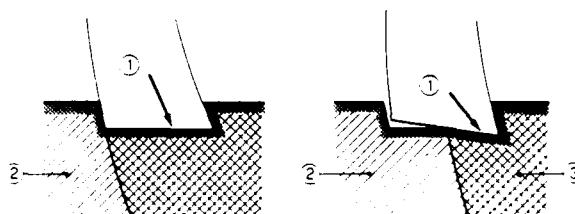


Fig. 34 Possible effect of a change in dam thrust

1. Dam thrust
2. Zone with extension strains
3. Zone with compression strains

When interpreting strain distribution curves in detail, one has to bear in mind that several factors are generally at work, that influence the deformation field. In the case of the Kölnbrein arch dam, the anisotropy of the rock may also affect the strain field. The present discussions were aimed at merely illustrating the nature of the information which can be obtained from strain distribution measurements. Therefore, no attempt was made to analyse the problems at the Kölnbrein arch dam as a whole. A detailed discussion of this problem is given elsewhere. It is conceivable that refined, two-dimensional finite element studies tailored to the specific rock conditions under individual blocks would largely support a correct interpretation of the measured deformations. Furthermore, they could also lead to an optimal arrangement of the measuring lines resulting in firm conclusions.

The Trivec probe was also used to detect and monitor structural deficiencies in the rock foundation of the dam. Fig. 35 shows some results of the Trivec measurements, carried out in block 17 of the dam body. The distribution of the differential displacements in horizontal (x) and vertical (z) direction due to the reservoir filling clearly shows the increase of intensity down to 15 m below the base of the dam (Amstad et al., 1987).

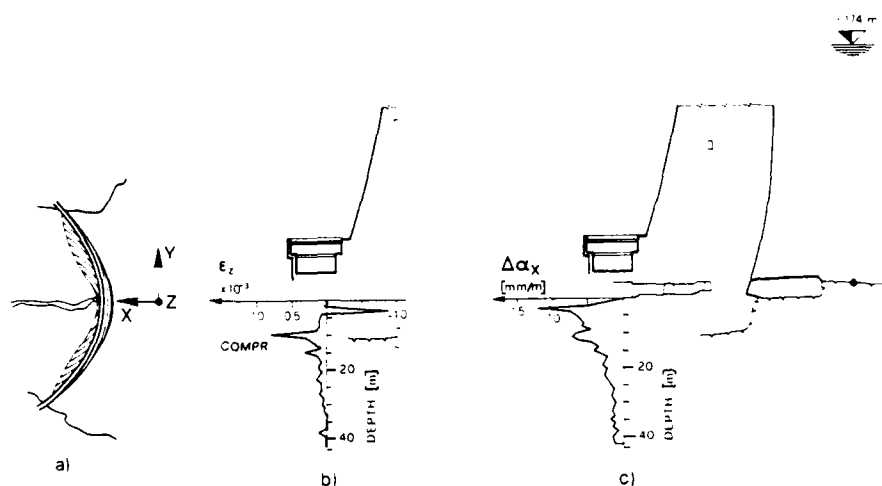


Fig. 35 Detection and monitoring of structural deficiencies in the foundation of the Kölnbrein dam

- a) Orientation of the coordinate system
- b) Strain development ϵ_z due to reservoir filling
- c) Change in inclination $\Delta\alpha_x$ due to reservoir filling

VALLE DI LEI ARCH DAM

This 141 m high arch dam with a crest length of 642 m is situated in the south eastern part of Switzerland at an altitude of 1800 m. The reservoir itself extends into Italian territory. The rock foundation consists of a moderately jointed sericit gneiss. In the central part of the dam a subhorizontal borehole was drilled in the down-stream direction in order to measure the pressure head distribution in the rock. For this purpose the Piezodex system was applied. This system involves eight monitoring sections with 1.50 m long single gas inflated packers and measurement intervals varying in length between 1.5 and 6.0 m. The packers were positioned in such a way that the measurement intervals covered the major fractures intersecting the borehole. At the time of the instrument installation, the reservoir level was at its maximum height and water flowed continuously from the borehole into the control gallery.

Readings were taken prior to the inflation of the packers, to check the field performance of the system under simple hydrostatic conditions. In Fig. 36, the obtained values are represented at full circles. All these points should theoretically lie on the horizontal line indicating the pressure head in the borehole according to the level of the mouth of the borehole. However, as the depth of the pressure transmitters was calculated, on the assumption of a straight drill-hole, the deviation of the points from the horizontal indicates local deviations of the drill-hole from its theoretical axis.

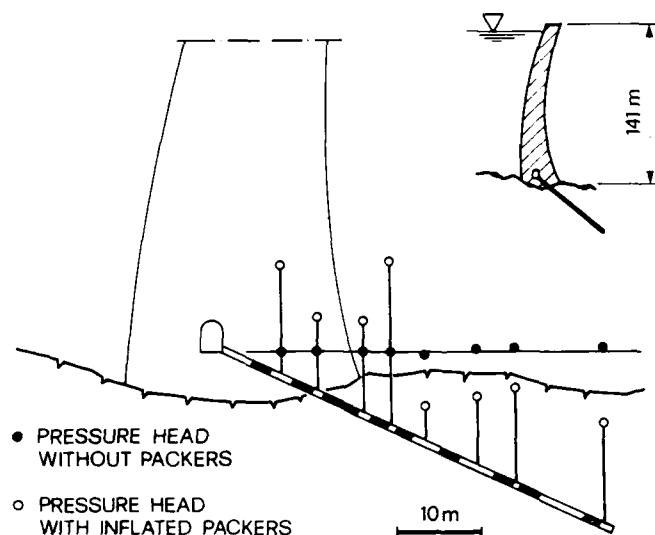


Fig. 36 Piezodex measurements in the foundation rock at Valle di Lei dam site immediately after installation

Once the packers had been inflated, the readings gave a completely different picture of the pressure head distribution along the borehole. In Fig. 37, results of readings which were taken at different reservoir levels in different seasons over the course of the two following years are represented. The piezometric heads at the borehole depths of 12, 19, and 22 m clearly correlate with season and with the reservoir levels. The other values do not appear to be influenced by the water level in the reservoir. The great difference in water pressure measured at adjacent measuring intervals (22 and 26.5 m) separated only by a 1.5 m long packer is remarkable. It shows how the nature of joint interconductivity may influence the distribution of water head in a moderately fractured rock mass. The interpretation of the results in Fig. 37 is made difficult by the presence of a grout curtain and probably much more by a set of drain holes also present in the area of the measuring line.

HEAD DISTRIBUTION IN THE ROCK FOUNDATION OF AN ARCH DAM (VALLE DI LEI)

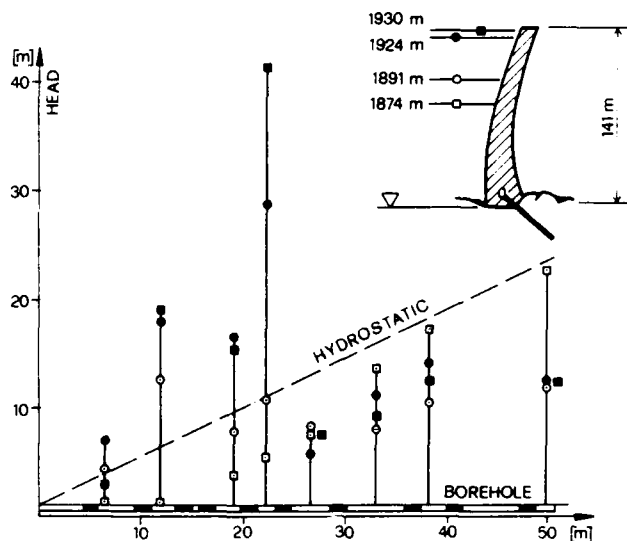


Fig. 37 Piezodex measurements at Valle di Lei dam site: head distribution at different reservoir levels in the course of two subsequent years

ALBIGNA GRAVITY DAM

The Albigna gravity dam is in the Southeast of the Swiss Alps, at an elevation of 2000 m (Fig. 38). The storage capacity of the reservoir is $67 \times 10^6 \text{ m}^3$, and the total head at the machine house, 6.5 km to the north, is 741 m. The dam has a crest length of 760 m and consists of blocks of 20 m breadth. The largest block in the middle of the valley is 115 m high (Fig. 39). Between the blocks there are joint spaces 5 m wide intended to reduce uplift at the dam base. One can, therefore, speak of a hollow-joint gravity dam. The rock foundation consists of a sound, coarse-grained granite of high strength. It exhibits three regular sets of joints. The distance between the joints varies between 1 and 10 m. The material filling is crystalline which leads to healed joints with a high filling strength. This is of great importance with regard to the deformation and strength properties as well as to the permeability of the rock mass.

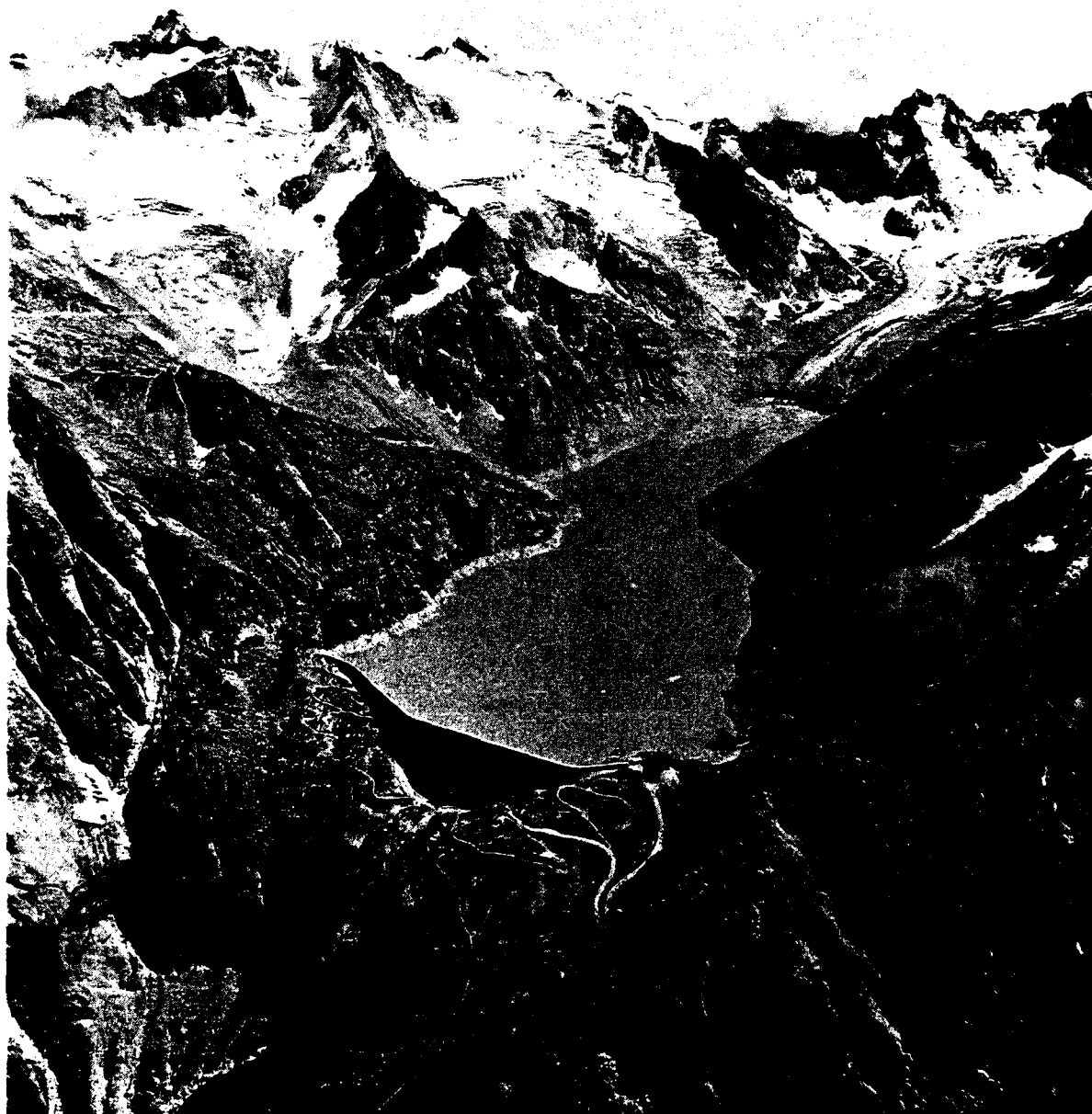


Fig. 38 Aerial view of the Albigna Gravity Dam (courtesy of Wild, Heerbrugg)

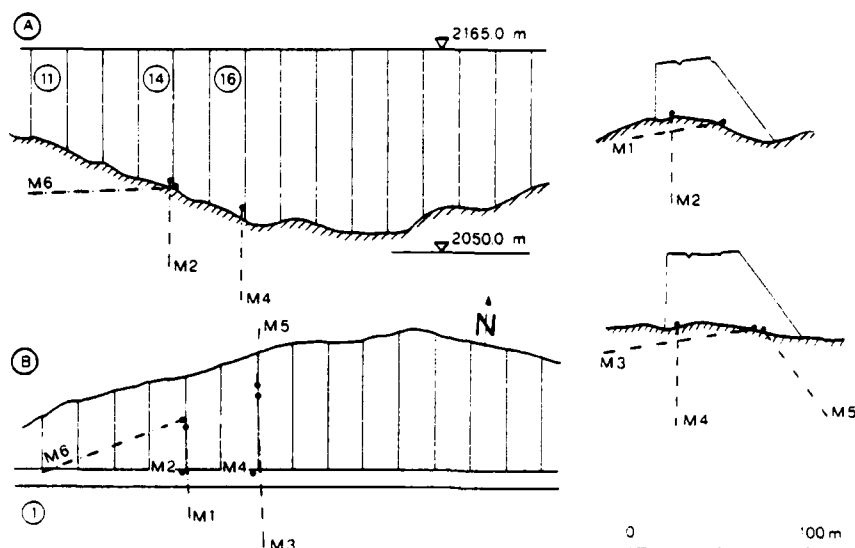


Fig. 39 Albigna Gravity Dam with boreholes for strain monitoring

A. Front view

B. Plan

1. Upstream face

In the planning and design stages, and also during construction in the period 1956-59, the foundation rock was considered to be very favourable. Neither the permeability nor the strength of the rock mass were regarded as presenting problems for the selected dam type. However, already during the first reservoir filling, in the summer of 1960, a clearly visible crack occurred in block 11 continuing in a filled rock joint. In the course of the years, some other unexpected events have happened, involving increasing water loss and a slight increase of permanent deformations. During the subsequent investigations, an open joint in the rock running along the upstream heel of the dam was detected. The joint, belonging to one of the principal joint sets, extended over a length of 300 m and its aperture was found locally to be up to 8 mm for the empty reservoir condition. This observation gave rise to an intensification of the investigations to obtain a clear picture of the processes taking place in the rock foundation, in order to develop the correct strategy for remedial measures. Their objective were to stop the underseepage and the tendency to increase deformations.

The actual condition of the dam could not be described as critical in any phase of the investigations during this period. The aim was to bring to a standstill a detrimental process which had fully been recognized at a very early stage. Measures had to be taken to prevent the development of new joint openings and the further propagation of the existing cracks. Of great importance was the prevention of water percolation into the rock foundation below the dam. However, although the aim was clearly defined, uncertainties existed concerning the following important questions:

- were there other joints parallel to this longitudinal crack, which would terminate perhaps under the alluvium deposit in the reservoir basin?
- what was their extent along the dam axis and in depth?
- were there further extensive open fissures in the rock belonging to one of the principal joint sets?

The last question was of special interest for wedge stability investigations. In this context, it should be remembered that the joint were filled with solid crystalline material which can, however, exhibit only a low tensile strength.

Answers to these questions were sought with the aid of systematic high precision rock deformation measurements.

Measurement Results:

Strain monitoring in the foundation rock was performed along six boreholes shown in Fig. 39. The length of these boreholes varied between 50 and 85 m, with a total length of 400 m. The orientation of the boreholes is such that they steeply intersect the principal sets of discontinuities.

Before going into details of the interpretation of measurement results, it should be emphasized that the most important finding of the measuring campaign was the detection of the peaks in the strain distribution. It very soon became obvious that only a few active joints requiring special attention were present in the foundation rock of the Albigna dam. Thus, the rock mass below the dam behaves mainly as a homogeneous, monolithic body. The active joint designated by A and B in Fig. 40 belongs to a principal joint set. The joint A intersects both the subhorizontal measuring line (M3) and the vertical ones (M2 and M4). Joint A is identical to the longitudinal crack discovered at an early stage of the investigations. The Sliding Micrometer measurements just confirmed its existence at depth and gave an indication as to the amount of its opening and closing due to the fluctuations of the reservoir level.

The active joint B was detected by the strain measurements (Fig. 41). After the removal of a mud layer from the reservoir floor adjacent to the toe of the dam, a set of longitudinal cracks on the rock surface which were obviously associated with the open joint B could be observed.

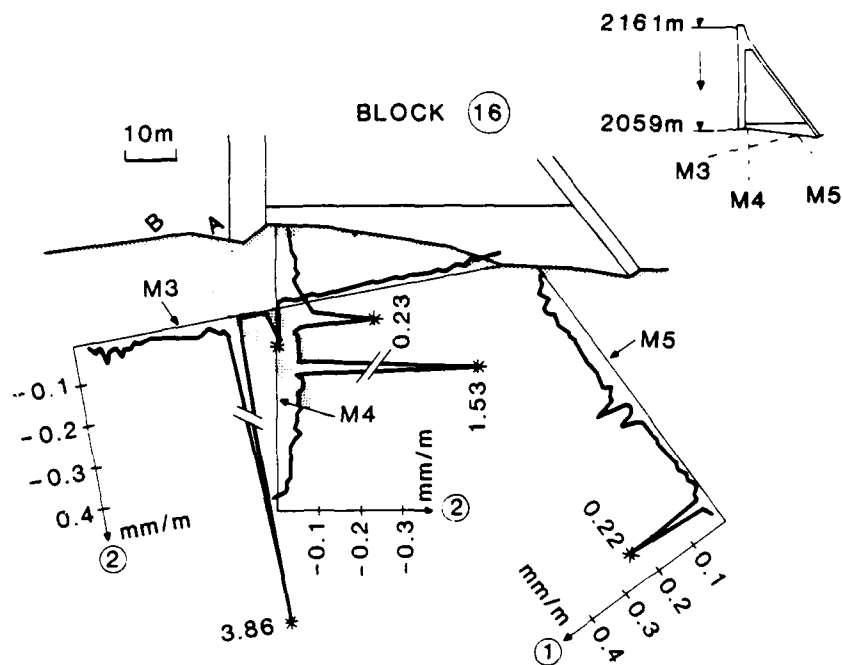


Fig. 40 Strain development due to fall in water level

- 1. Extension strain
- 2. Compression strain
- A. Active joint
- B. Active joint

The question of whether only one joint or more of them opened and closed within the 1 m base length of the measurements, causing a deformation of 3.86 mm/m is of no particular relevance. The three boreholes, M3, M4, and M5 at block 16 (Fig. 39) give an almost complete picture of the deformational behaviour of the bedrock. Apart from the peaks, the strain distribution reveals the normal behaviour of the rock as well. The occurrence of only a few active joints and the high rigidity of the rock mass confirmed the excellent overall rock conditions at the Albigna dam site. The remedial measures to stop the underseepage of the dam were carried out in the summer of 1980. A more detailed discussion of the Albigna dam is given elsewhere (Kovari and Peter, 1983).



Fig. 41 Longitudinal cracks (system B) on the rock surface at the upstream toe of the dam seen after removal of mud

EXAMPLE OF A CREEPING SLOPE

A large subsidence mass near the village of Klosters in the eastern part of Switzerland has been continuously monitored by geodetic measurements over the last 50 years. This has shown a rate of displacement of 50 mm per year. There are several interesting geotechnical problems related to this slope, one of which concerns the project study for a bypass of Klosters. The geological structure of the subsidence mass is not well-known yet. The main, overlying part (Fig. 42) consists of a loosened rock zone of moraine and rubble material which is wet but, due to its low permeability, very difficult to drain. It is assumed that creeping started several thousand years ago and was not preceded by a slide.

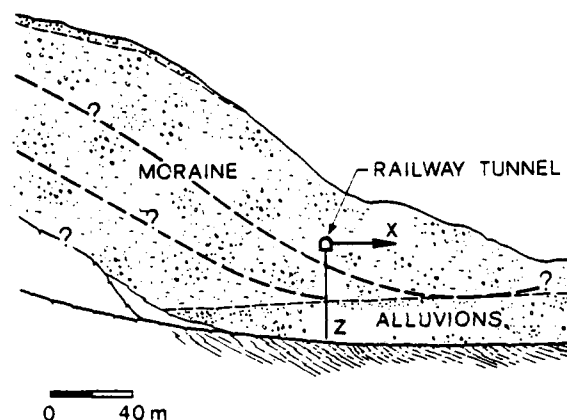


Fig. 42 Geological section through the subsidence mass with one of the Trivec boreholes below a railway tunnel near Klosters

The information obtained from Trivec measurements (Amstad et al., 1987) was to determine the displacement field in the slope below the railway tunnel, in order to find the presence of a distinct sliding surface, if any. It was also intended to determine the inclination of such possible sliding surfaces from the measured displacement vectors.

The results (Fig. 43) yield a clear picture of what is going on in the slope. Obviously, there are two distinct sliding surfaces revealed by the sharp peaks in the distribution of the change in inclination $\Delta\alpha_x$. They are located at 10 and 20 m, respectively, below the tunnel. The strain distribution also shows peaks at the same locations, thus pointing to a compression of the zones where sliding occurs. Furthermore, the movements here take place almost only in a horizontal direction, as shown by the corresponding displacement vectors. We may therefore conclude that the sliding surfaces intersecting the borehole are nearly horizontal. This is an invaluable piece of information which could have been difficult to obtain otherwise.

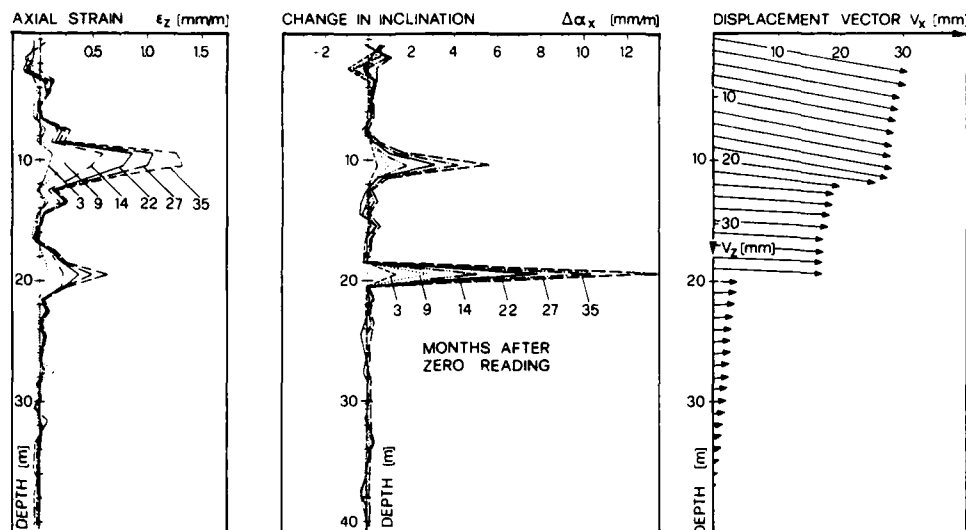


Fig. 43 Displacement field in a creeping slope 35 months after zero reading (after Amstad et al., 1987)

- distribution of the axial strain
- change in inclination in the dip direction of the slope
- displacement vectors along the borehole axis in the xz-plane

A noticeable creep deformation in the slope, indicated by the approximately linear increase of the magnitude of the displacement vector from the bottom of the drillhole to its mouth, is also superimposed on the sliding movements. The diagram of the $\Delta\alpha_x$ -distribution shows that the slip of the two rock layers between 0 and 10 m and between 10 and 20 m occurs within two measuring marks of the Trivec casing, i.e. within a soil layer of 2.0 m. We do not know whether the shear movement is confined to an even narrower area. It is more important to realize that the rates of shear displacement $\Delta\alpha_x$ at these locations are almost constant, having values of 1.9 mm/year and 4.6 mm/year respectively (Fig. 44).

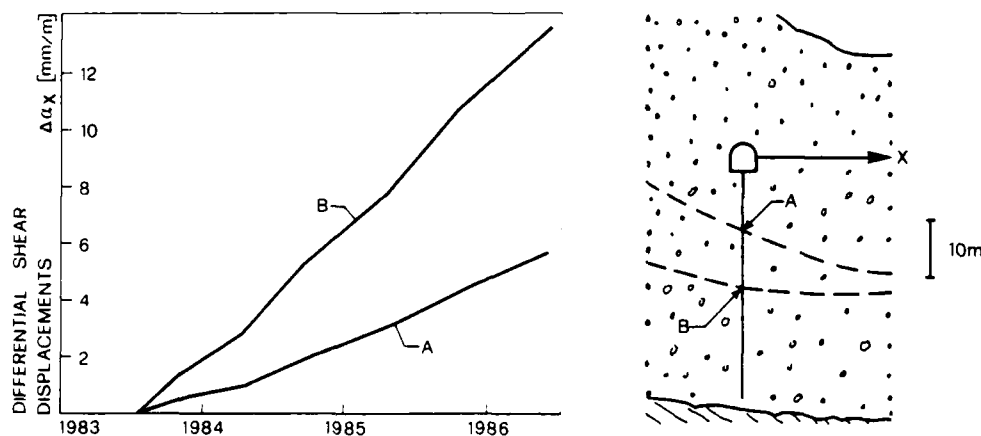


Fig. 44 Rates of differential shear displacements on two sliding surfaces in the dip direction versus time (after Amstad et al., 1987)

References

- Amstad, Ch., Köppel, J., Kovari, K. (1987): Trivec Measurements in Geotechnical Engineering. Proc. 2nd Int. Symposium on Field Measurements in Geomechanics, Kobe, Japan, Balkema Publishers.
- ASCE/USCOLD (1975): Lessons from Dam Incidents, USA.
- Baustädter, K., Wiedmann, R. (1974): The behaviour of the Kölnbrein Arch Dam. Transactions of the 15th Int. Congress on Large Dams, Lausanne.
- Biedermann, R. (1985): Dam Safety in Switzerland. Swiss Dams, Monitoring and Maintenance, Swiss National Committee on Large Dams.
- Bishop, A.W. (1955): The use of the slip circle in the stability analysis of slopes. Géotechnique, v.5, no. 1.
- Burmister, D.M. (1946): Factor of safety in stability analysis. Civil Engineering, v.16, no. 7.
- Chen, W.F. (1975): Limit analysis and soil plasticity. Elsevier Amsterdam.
- Chen, W.F., Morgenstern, N.R. (1981): Extensions to the Generalized Method of Slices for Stability Analysis. Canadian Geotechnical Journal.
- Groupe de Travail du CFGB (1970): Quelques développements de moyens d'auscultation du massif rocheux. ICOLD, 10th Int. Congress, Montréal.
- ICOLD (1974): Lessons from Dam Incidents.
- ICOLD (1978): Finite Element Methods in Analysis and Design of Dams, Bulletin 30.
- ICOLD (1987): Dam Safety Guidelines, Bulletin 59.
- Janbu, N. (1954): Application of composite slip surfaces for stability analysis. Proc. Europ. Conf. Stability Earth Slopes, v.3, pp. 43 - 49.
- John, K.W. (1976): Felsgründungen von grossen Talsperren, Probleme Lösungen. Rock Mechanics, Suppl. 5., pp. 61-79.
- Köppel, J., Amstad, Ch., Kovari, K. (1983): The Measurement of Displacement Vectors with the "Trivec" Borehole Probe. Proc. Int. Symposium on Field Measurements in Geomechanics, Zürich, Balkema Publishers.
- Kovari, K., Amstad, Ch. (1983): Fundamentals of Deformation Measurements. Proc. Int. Symposium on Field Measurements in Geomechanics, Zürich, Balkema Publishers, Vol. 1, pp. 219-239.
- Kovari, K., Amstad, Ch., Köppel, J. (1979): New Developments in the Instrumentation of Underground Openings. RETC Proc. Rapid Excavation and Tunnelling Conf., Atlanta, Vol. 1, pp. 817-837.
- Kovari, K., Fritz P. (1976): Stabilitätsberechnung ebener und räumlicher Felsböschungen. Rocks Mechanics, v.8, No. 2.
- Kovari, K., Fritz P. (1978): Slope stability with plane, wedge and polygonal sliding surfaces. Int. Symp. Rock Mech. related to Dam Foundations, Rio de Janeiro.
- Kovari, K., Köppel, J. (1987): Head Distribution Monitoring with the "Piezodex" Sliding Piezometer System. 2nd Int. Symposium on Field Measurements in Geomechanics, Kobe, Japan, Balkema Publishers.

- Kovári, K., Peter, G. (1983): Continuous Strain Monitoring in the Rock Foundation of a large Gravity Dam. Rock Mechanics and Rock Engineering, Vol. 16, No. 3, pp. 157-171.
- Londe, P. (1973): Rock Mechanics and Dam Foundation Design, ICOLD Publication.
- Londe, P. (1977): Field Measurements in Tunnels. Proc. Int Symposium on Field Measurements in Rock Mechanics, Zürich, Vol. 2, pp. 619-638.
- Londe, P. (1978): Foundations and Slope Treatment. Proc. Int. Symposium on Rock Mechanics Related to Dam Foundations, Rio de Janeiro, pp. V.1 - V.68.
- Magnet, E., Widmann, R. (1974): Gründungsprobleme der Gewölbemauer Kölnbrein. Proc. 3rd ISRM Congress, Denver, USA, Vol. 11, Part B, pp. 902-907.
- Morgenstern, N.R., Price, V.E. (1965): The analysis of the stability of general slip surfaces. Géotechnique, v.15, 1, pp. 79 - 93.
- Patton, F.P. (1979): Groundwater Instrumentation for Mining Projects. Proc. 1st Int. Mining Drainage Symposium, Denver.
- Rescher, O.J. (1981): Geomechanische Modelluntersuchungen für die Gründung von Talsperren. Rock Mechanics, Vol. 14, pp. 117-166.
- Rocha, M. (1978): Analysis and Design of the Foundation of Concrete Dams. Proc. Symp. Rock Mech. related to Dam Foundations, Rio de Janeiro, Brazil.
- Sarma, S.K. (1979): Stability Analysis of Embankments and Slopes. Journ. Geotechn. Engng. Div., GT12.
- Sultan, H.A., Seed, B.H. (1967): Stability of sloping earth dams. Proc. ASCE, SM4.
- Taylor, D.W. (1948): Fundamentals of soil mechanics. J. Wiley, New York.
- von Thun, J.L. (1977): Report on the Evaluation of Static Stability. Proc. of the Conference on the Evaluation of Dam Safety, ASCE.

END

DATE

FILMED

DTIC

9-88